

## Review

---

# Quantum Correlation Resource Recycling via Sequential Measurements: Theoretical Models and Optical Experiments

---

Xianzhi Huang, Liyao Zhan, Liang Li, Suhui Bao, Zipeng Tao and Jiayu Ying

## Special Issue

Quantum Optics: Science and Applications

Edited by

Dr. Hua-Lei Yin, Dr. Peng Xu and Dr. Jie Chen

Review

# Quantum Correlation Resource Recycling via Sequential Measurements: Theoretical Models and Optical Experiments

Xianzhi Huang <sup>1,\*</sup>, Liyao Zhan <sup>1</sup>, Liang Li <sup>2</sup>, Suhui Bao <sup>2</sup>, Zipeng Tao <sup>3</sup> and Jiayu Ying <sup>3</sup>

<sup>1</sup> Institute for Quantum Technology and Engineering Computing, School of JiaYang, Zhejiang Shuren University, Hangzhou 310015, China; zhanliyao@zjsru.edu.cn

<sup>2</sup> College of Biological and Environmental Engineering, Zhejiang Shuren University, Hangzhou 310015, China

<sup>3</sup> College of Information Science and Technology, Zhejiang Shuren University, Hangzhou 310015, China

\* Correspondence: huangxianzhi@zjsru.edu.cn

**Abstract:** Quantum correlation is a key resource for a variety of quantum information processing and communication tasks, the efficient utilization of which has been a longstanding concern, and it is also one of the main challenges in the application of quantum technology. In this review, we focus on the interaction between quantum measurements and quantum correlations by designing appropriate measurement strategies, specifically exploring the trade-off between information gain and disturbance degree in weak measurements to ensure that quantum correlations from the same source can be shared among multiple independent observers. We introduce the basic knowledge and classification of quantum measurements, investigate the weak measurement scenario, and show the theoretical model construction of quantum correlation recycling in the original works. We summarize the theoretical and experimental development process and the latest progress in this field. Finally, we provide an outlook for more quantum resource applications that can profit from the optimization of quantum measurement strategies.

**Keywords:** quantum correlation recycling; weak measurement; Bell nonlocality; quantum random number; optical setup



**Citation:** Huang, X.; Zhan, L.; Li, L.; Bao, S.; Tao, Z.; Ying, J. Quantum Correlation Resource Recycling via Sequential Measurements: Theoretical Models and Optical Experiments. *Photonics* **2023**, *10*, 1314. <https://doi.org/10.3390/photonics10121314>

Received: 1 November 2023

Revised: 24 November 2023

Accepted: 27 November 2023

Published: 28 November 2023



**Copyright:** © 2023 by the authors. Licensee MDPI, Basel, Switzerland. This article is an open access article distributed under the terms and conditions of the Creative Commons Attribution (CC BY) license (<https://creativecommons.org/licenses/by/4.0/>).

## 1. Introduction

Quantum correlation is the cornerstone in the field of quantum fundamental problems, and a property that is different from the locality and reality intuition of the macro world has attracted wide attention. Two particles at a certain distance can share an entanglement state to establish quantum correlations [1,2], specific forms of which are quantum entanglement, EPR (Einstein–Podolsky–Rosen) steering, and Bell nonlocality, constituting three quantum correlation hierarchies from weak to strong [3,4]. For illustration, we can demonstrate the general form of a two-qubit entangled state as

$$|\Psi\rangle = a|00\rangle + b|01\rangle + c|10\rangle + d|11\rangle, \quad (1)$$

where  $a$ ,  $b$ ,  $c$ , and  $d$  are complex coefficients satisfying  $|a|^2 + |b|^2 + |c|^2 + |d|^2 = 1$ , and  $|00\rangle$ ,  $|01\rangle$ ,  $|10\rangle$ ,  $|11\rangle$  represent the ground states of two qubits, respectively. For the above bipartite scenarios from quantum entanglement to nonlocality, the entanglement of an unknown state  $\rho_{AB}$  is certified by a sequence of semi-definite programs (SDP) [5], a single SDP test [6], and a linear program [3]. It can be concluded that EPR steering is a form of quantum correlation, of which the corresponding test can be seen as a scenario lying in between the nonlocality test [3] and standard entanglement test [7,8].

In addition, quantum discord [9], as a complementary form of quantum correlations, has been shown to exist in the absence of quantum entanglement. A recent study [10] has also experimentally realized a form of quantum correlation that does not require the premise of entanglement and discord. For single-particle systems, more attention

has been paid to the quantum correlation between multiple commutative measurements, that is, the contradiction between noncontextual realism and quantum theory proved by Kochen and Specker (KS) [11], also known as quantum contextuality. These multiple forms of quantum correlations reveal the difference between quantum mechanics and classical mechanics, and give rise to disciplines such as quantum information and quantum computing, which have important application potentials in quantum teleportation [12], quantum key distribution [13], quantum dense coding [14], quantum secret sharing [15], quantum digital signatures [16], quantum conference key agreement [17], and multi-party quantum network [18–21].

All quantum correlations, in essence, are monogamous: when there are multiple observers, the limit on quantum correlation sharing is quantitatively expressed as a one-to-one relationship [22–25]; i.e., two observers cannot simultaneously prove quantum correlations with a third observer. This restriction makes it difficult to utilize quantum correlation resources effectively. To overcome this difficulty, the effect of quantum measurement might be considered. Unlike classical measurements, quantum measurements inevitably disturb the target system [26], and, when projective measurements are manipulated, the system collapses into the eigenstates of observables [27]. This method of measurement guarantees the maximum amount of information extracted, but also unquestionably breaks quantum correlations. In contrast, other measurement schemes, such as weak measurements, despite obtaining only part of the system information, can still retain some quantum correlation corresponding to the degree of disturbance to the system [28–30]. Therefore, considering the trade-off between the degree of disturbance to quantum states and information gain by measurements [31–33], it provides inspiration for exploring the recycling of quantum correlations.

In 2015, Silva et al. [34] started by studying the trade-off between information gain and disturbance of a von Neumann-type measurement. They define the measurement quality factor  $F$  (which represents the preservation of original states) and precision  $G$  (which represents the ability to obtain measured state information), respectively. By adjusting the relative strength of these two parameters and applying this model to quantum nonlocality problems, it is proposed that an entangled pair can be shared by multiple observers measuring sequentially that are independent of each other. If two observers are represented by Alice and Bob, then Alice will be quantum-correlated to more than one Bob. It should be noted that this situation does not give rise to arguments about monogamous relationships because, in the above scenario,  $\text{Bob}_1$  implicitly signals to  $\text{Bob}_2$  by choosing its measurement settings, so the no-signaling condition in the sequential measurement is relaxed without violating relativistic causality [35]. This study is pioneering in showing that quantum correlations from an entangled pair can be recycled in the sequence of independent observers. As an efficient way to use quantum resources, this trade-off both guarantees enough information extraction to violate classical bounds and preserves enough correlations for subsequent independent quantum information tasks. Building on the above results, recent theoretical research has focused on the areas of entanglement witness, EPR steering, quantum contextuality, and, most famously, Bell nonlocality. Noteworthy application work is also investigated in the field of quantum randomness extraction, which builds a natural scenario for certified quantum instruments and is an important resource in scientific simulation and cryptography [36–38]. In terms of experimental verification, a variety of research teams have also continuously proposed new achievements in the direction of quantum correlation recycling, most of which rely on optical platforms. These works extensively discuss the quantum correlation sharing in different sequential weak measurement scenarios, where adjustable parameters include, but are not limited to, input qubit biases, the sharpness of different measurement settings, and one-sided/two-sided sequences, which are of great significance for efficient utilization of quantum correlations. The quantum correlation recycling experiments currently implemented in optical setups are also conducive to the development of emerging quantum technology at the practical and application level and provide guidance for other important qubit platforms, such as solid-state qubits [39,40].

This review summarizes and discusses the theoretical and experimental developments in quantum correlation recycling under sequential weak measurements, aiming to provide readers with more insights on quantum resource utilization based on different measurement strategies. The structure of this review is as follows. In Section 2, we introduce the theory of measurement in quantum physics and describe the differences and connections between general measurement, projective measurement, and POVM measurement, paving the way for introducing the concept of weak measurement. In Section 3, we learn from the works of Silva et al. [34] and Mal et al. [41], who mainly demonstrate the original scenario of quantum correlation sharing among multiple observers under weak measurements, deduce the theoretical models, and show the numerical results. Next, in Section 4, we summarize the progress in theoretical exploration and experimental verification regarding the direction of quantum correlation recycling under sequential measurements, and then make some brief comments. The discussion part is in Section 5; we present a table to exhibit the main theoretical progress mentioned in the review and further discuss the relevant applications and experiments. The latest development in the projection measurement strategy is also introduced. Finally, we look forward to the reality that utilization of quantum resources will benefit further from the design of measurement strategies in Section 6.

## 2. Measurement in Quantum Physics

For a given quantum system, we need to understand what is going on inside through the operation of observation, which is specifically called “quantum measurement”. The interpretation of quantum measurement is the core problem in the construction of quantum physics [42,43], and also the application basis of quantum information and quantum computing fields. The general description of quantum measurement is based on the following assumption [44]: a group of operators  $\{M_m\}$  represents measurements upon the Hilbert space associated with an observed physical system, where subscript  $m$  indicates possible measurement results. If the most recent state of this quantum system before measurement is  $|\psi\rangle$ , then the probability for the outcome  $m$  is provided by

$$p(m) = \langle\psi|M_m^\dagger M_m|\psi\rangle, \quad (2)$$

while the quantum state is updated to

$$|\psi\rangle \rightarrow |\psi'\rangle = \frac{M_m|\psi\rangle}{\sqrt{\langle\psi|M_m^\dagger M_m|\psi\rangle}}. \quad (3)$$

Measurement operators satisfy the completeness condition:  $\sum_m M_m^\dagger M_m = I$  and naturally guarantee that the sum of probabilities for possible outcomes is equal to 1.

In particular, if operators  $\{M_m\}$  in the above general measurement also meet the requirements for orthogonal projection operators, which means

1.  $\{M_m\}$  are Hermitian,  $M_m = M_m^\dagger$ ;
2.  $\{M_m\}$  satisfy  $M_m M_{m'} = \delta_{m,m'} M_m$ ,
- and their derivative properties
3.  $\{M_m\}$  are positive semi-definite matrices;
4.  $\{M_m\}$  are idempotent:  $M_m^2 = M_m = M_m^n$ ,

we can define von Neumann, or projective measurement with these additional constraints. For a given state  $|\psi\rangle$ , the projection operator is specified by  $P_m = |\psi_m\rangle\langle\psi_m|$ , and the probability of obtaining the measurement outcome  $m$  is

$$p(m) = \langle\psi|P_m|\psi\rangle, \quad (4)$$

where the post-measurement quantum state is described by

$$|\psi\rangle \rightarrow |\psi'\rangle = \frac{P_m|\psi\rangle}{\sqrt{p(m)}}. \quad (5)$$

Here, the projection operator  $P_m$  and corresponding outcome  $m$  constitute the spectral decomposition of the observable mechanical quantity  $M$  upon the above quantum state space, that is

$$M = \sum_m m P_m. \quad (6)$$

For any observable  $M$ , the measurement expectation value for a quantum state can be calculated by

$$\langle M \rangle = \text{tr}(M\rho), \quad (7)$$

where  $\rho$  is the density matrix corresponding to a pure or mixed state. From the mathematical expression of projection measurement, we can easily obtain its repeatability; that is, a projection operation  $P_m$  will obtain an outcome  $m$ , and the measurement result remains unchanged after repeatedly applying  $P_m$  to the quantum state. The above point suggests that projection measurement is significantly different from general measurement because the latter usually destroys the quantum state and makes the corresponding result unrepeatable.

However, if we ignore the description of the post-measurement quantum state in the specific application scenario and only care about the possibility of obtaining different outcomes from the measurement, a mathematical tool named positive-operator-valued measure (POVM) is generalized [44,45]. In a POVM measurement, the new set of Hermitian operators  $\{E_m\}$  is defined as

$$E_m = M_m^\dagger M_m, \quad (8)$$

and it is obvious that  $\{E_m\}$  are positive semi-definite operators satisfying  $\sum_m E_m = I$  and  $p(m) = \langle \psi | E_m | \psi \rangle$ . Each operator  $E_m$  is referred to as a POVM element related to the outcome  $m$ , and a complete set of  $\{E_m\}$  defines a POVM. In essence, POVM measurements do not introduce new concepts in physics but can be viewed more as a simple and convenient mathematical approach just to provide additional inspiration for studying the statistical properties of general measurements.

Now, let us discuss the relationship between these different types of measurement settings. A projection-valued measure (PVM) defined by a set of projection operators  $\{P_m\}$  is a special case of POVMs, in which each element of this POVM satisfies the equation:  $E_m = P_m^\dagger P_m = P_m$ . For PVMs, the projectors  $\{P_m\}$  have rank 1, which is not necessary for POVMs. However, Neumark's theorem [46,47] demonstrates the way to achieve POVMs through PVMs acting on a higher dimension space, and here we discuss the brief explanation of this theorem in two cases of POVM operators:

- Rank = 1: a set of un-normalized vectors  $\{e_i\}$  satisfying  $\sum_{i=1}^k |e_i\rangle\langle e_i| = I$

Considering an  $n$ -dimension space ( $n \leq k$ ), the above  $k$  un-normalized vectors can construct a  $n \times k$  matrix  $M$ , and each element  $M_{i,j}$  corresponds to the  $i$ th coordinate of  $|e_j\rangle$ , written as  $\langle i|e_j\rangle$ . Next, we calculate the inner product of row  $i$  and  $i'$  to prove orthogonality, that is

$$\begin{aligned} \sum_{j=1}^k \langle i|e_j\rangle\langle e_j|i'\rangle &= \langle i|(\sum_{j=1}^k |e_j\rangle\langle e_j|)|i'\rangle \\ &= \langle i|i'\rangle \\ &= \delta_{i,i'}. \end{aligned} \quad (9)$$

Thus, we obtain  $n$  orthogonal rows within a  $k$ -dimension space, and the next step is to extend the number of rows from  $n$  to  $k$  using the Gram-Schmidt process. Since this  $k \times k$  square matrix  $M'$  is unitary:  $M'M'^\dagger = I_k = M'^\dagger M'$ , we can rewrite  $M'$  in the form of orthogonal columns:

$$M' = \{|p_1\rangle, |p_2\rangle, \dots, |p_k\rangle\}, \quad (10)$$

and each column of this new matrix  $M'$  can construct a projector  $P_i = |p_i\rangle\langle p_i|$  forming a PVM  $\{P_i, i = 1, 2, \dots, k\}$ , while the original  $n$ -dimensional subspace defines the above POVM with rank-1.

- Rank  $> 1$ : a set of Hermitian operators  $\{E_i\}$  satisfying  $\sum_i E_i = I$

The set  $\{E_i\}$  can be diagonalized using the spectral theorem:

$$E_i = \sum_j \lambda_{ij} |f_{ij}\rangle\langle f_{ij}| = \sum_j |e_{ij}\rangle\langle e_{ij}|. \quad (11)$$

Here,  $\lambda_{ij}$  and  $|f_{ij}\rangle$  are eigenvalues and eigenvectors of the matrix  $E_i$ , while  $|e_{ij}\rangle = \sqrt{\lambda_{ij}}|f_{ij}\rangle$ . Thus, we can turn this problem into the case of rank-1 and transform the POVM  $\{E_i\}$  to a projective measurement  $\{P_i\}$  formulated by orthogonal vectors  $\{|p_{ij}\rangle\}$  in the higher dimension space. The above two cases fully demonstrate that POVMs can be physically realized by PVMs with the higher dimension in practical measurements, whose result is crucial in quantum physics [48].

For PVMs and general measurements, we introduce a complex quantum system  $Q_1 \otimes Q_2$  and define a unitary operator  $U$  working on the state  $|\psi\rangle_1|0\rangle_2$ :

$$U|\psi\rangle_1|0\rangle_2 = \sum_m M_m |\psi\rangle_1|m\rangle_2. \quad (12)$$

After that, we propose the projective measurement  $P_m = I_1 \otimes |m\rangle\langle m|_2$ , and the probability for obtaining the outcome  $m$  is

$$\begin{aligned} p(m) &= \langle\psi|_1\langle 0|_2 U^\dagger P_m U |\psi\rangle_1|0\rangle_2 \\ &= \sum_{m',m''} \langle\psi|_1\langle m'|_2 M_{m'}^\dagger (I_1 \otimes |m\rangle\langle m|_2) M_{m''} |\psi\rangle_1|m''\rangle_2 \\ &= \langle\psi|_1 M_m^\dagger M_m |\psi\rangle_1, \end{aligned} \quad (13)$$

while the post-measurement quantum state for the system  $Q_1$  becomes

$$|\psi\rangle \rightarrow |\psi'\rangle = \frac{M_m |\psi\rangle}{\sqrt{\langle\psi| M_m^\dagger M_m |\psi\rangle}}. \quad (14)$$

As we can see, after introducing additional auxiliary systems, projective measurements under the unitary operation are equivalent to general measurements of any form. Moreover, in complex quantum systems, there exists one of the most magical properties of quantum physics, entanglement, whose interaction with quantum measurements will be discussed further in the next section.

### 3. Bell NonLocality Sharing: The Unsharp Measurement Formalism

Entanglement is a marvelous phenomenon in a complex quantum system [1,49], and its anticlassical property not only questions the description of local realism in classical physics [2] but also provides a key quantum resource for surpassing classical computing power [8]. For a given quantum resource, how to better achieve recycling is also very important to ensure the effective use of quantum technology. Among them, the design of a quantum measurement scheme provides an effective idea for this quantum correlation sharing by multiple independent observers, especially in the sequential network.

The original scenario [34] was first introduced by investigating the trade-off between the information gain and disturbance upon the entangled states. The generalization from projective measurements to general forms can be achieved by investigating von Neumann-type measurement pointers [27] for spin- $\frac{1}{2}$  particles: the system to be measured is called the *target*, while the measurement *pointer* system is prepared independently and then interacts with the target. By performing quantum measurements upon the pointer, the information of the target can be obtained. For a von Neumann-type measurement, the initial state of the target and pointer is therefore

$$|\Psi\rangle_{tar} \otimes |\varphi(q)\rangle_{poi}, \quad (15)$$

while the post-measurement state is described using the coupling constant  $g_0$

$$\sum_a \langle a | \Psi \rangle \cdot |a\rangle_{tar} \otimes |\varphi(q - g_0 a)\rangle_{poi}. \quad (16)$$

Here, we take the index  $a$  to denote a set of basis states for the measured target observable and the drift of position parameter  $q$  to indicate the measurement outcome. For simplicity, we set  $g_0 = 1$ . For a strong or projective measurement, the initial state of pointer is narrow enough to distinguish different eigenvalues, which means

$$\langle \varphi(q - a) | \varphi(q - a') \rangle = \delta_{aa'}, \quad (17)$$

so that the position of the pointer after measurement can fully reflect the information of measured physical system and project the target quantum state onto the corresponding eigenstate  $|a\rangle$ .

However, if considering the opposite case that the spread of pointer is extremely wide to cover the whole spectrum of eigenvalues, we cannot obtain the target system information by reading the post-measurement position of the pointer. In the above scenario,

$$\begin{aligned} \langle \varphi(q - a) | \varphi(q - a') \rangle &\approx 1 \rightarrow |\Psi'\rangle_{|q_0} = \sum_a \langle a | \Psi \rangle \langle q_0 | \varphi(q - a') \rangle |a\rangle \\ &\approx \langle q_0 | \varphi(q) \rangle \sum_a \langle a | \Psi \rangle |a\rangle \\ &= \langle q_0 | \varphi(q) \rangle |\Psi\rangle, \end{aligned} \quad (18)$$

which leaves the target quantum state undisturbed and defines the limit for a weak or nonprojective measurement.

Now, let us discuss measurement schemes between the above two extremes: taking spin- $\frac{1}{2}$  particles, for example, the initial state for target system is linear combination of eigenstates corresponding to the measured observable, that is  $|\Psi\rangle = \alpha|\uparrow\rangle + \beta|\downarrow\rangle$ ; thus

$$|\Psi\rangle \otimes |\varphi(q)\rangle \rightarrow \alpha|\uparrow\rangle \otimes |\varphi(q - 1)\rangle + \beta|\downarrow\rangle \otimes |\varphi(q + 1)\rangle. \quad (19)$$

The post-measurement state of target system is obtained after tracing over all position information of the pointer

$$\rho' = F|\Psi\rangle\langle\Psi| + (1 - F)(|\uparrow\rangle\langle\uparrow| |\Psi\rangle\langle\Psi| |\downarrow\rangle\langle\downarrow| + |\downarrow\rangle\langle\downarrow| |\Psi\rangle\langle\Psi| |\uparrow\rangle\langle\uparrow|). \quad (20)$$

Here, the parameter  $F$  is calculated using the displacement of pointer states

$$F = \int_{-\infty}^{+\infty} \varphi(q + 1) \varphi(q - 1) dq, \quad (21)$$

which reflects the effect of pointer initial state on the target post-measurement state and characterizes the proportion of original states avoiding to be decohered; hence, we label it as the “quality factor”.

Next, we turn to determine the measurement outcome through reading the pointer's positions, of which positive/negative results are associated with  $+1/-1$  outcomes from dichotomic spin values. The probabilities for reading the outcome  $+1$  are then provided by

$$p(+1) = G\langle\Psi||\uparrow\rangle\langle\uparrow||\Psi\rangle + (1 - G)\frac{1}{2}, \quad (22)$$

and a similar derivation leads to  $P(-1)$  under symmetry simplifications, i.e.,  $|\varphi(q)| = |\varphi(-q)|$ . The information gain, or labeled as the "precision" of measurements,  $G$  is calculated by

$$G = \int_{-1}^{+1} \varphi^2(q) dq. \quad (23)$$

Here,  $F$  and  $G$  are both independent of the spin state and able to co-describe a von Neumann-type measurement. For example,  $\varphi(q) = 1/(\sqrt{2\Delta})(-\Delta < q < +\Delta)$  in a square pointer state, and there are two cases that satisfy the following

$$\begin{aligned} &\text{if } \Delta \leq 1 \rightarrow \text{a strong measurement : } F = 0, G = 1; \\ &\text{or else } \Delta > 1 \rightarrow \text{a weak measurement : } G = 1 - F. \end{aligned} \quad (24)$$

However, this example does not achieve an optimal trade-off between  $F$  and  $G$ , nor the commonly used Gaussian wave packet. The calculation result shows that the optimal pointer distribution is related to the measurement precision  $G$

$$\begin{aligned} \varphi(q) &= f(q - 2n)(\sqrt{\frac{1-G}{1+G}})^{|n|} \\ \forall q &\in (2n - 1, 2n + 1], n \in \mathbb{Z}, \end{aligned} \quad (25)$$

and the trade-off is given by

$$F^2 + G^2 = 1. \quad (26)$$

Consider the Bell scenario shown in Figure 1a, in which Alice and Bob share a pair of entangled particles with spin- $\frac{1}{2}$  but, unlike usual, Bob performs two independent measurements sequentially. Now, for Alice–Bob<sub>1</sub> and Alice–Bob<sub>2</sub>, we will see if the nonlocality is maintained by testing the Bell-CHSH inequality [50]

$$I_{CHSH}^{(n)} = E_{00}^{(n)} + E_{01}^{(n)} + E_{10}^{(n)} - E_{11}^{(n)} \leq 2 \quad (27)$$

where  $E_{xy}^{(n)}$  is the correlation of measurement outcomes along the corresponding directions related to Alice's input  $x \in \{0, 1\}$  and each Bob's input  $y_n \in \{0, 1\}$ . A measure for the magnitude of Bell nonlocality is described by the violation visibility of Bell-CHSH inequality:  $V_n = I_{CHSH}^{(n)} - 2$ . It is worth noting that there is an implicit signal passing between Bob<sub>1</sub> and Bob<sub>2</sub> through the selection of measurement settings first, thus avoiding the conventional monogamy arguments for entanglement and nonlocality. The original article divided this Bell scenario into two cases according to the *input bias* of Bob<sub>1</sub>, which means the frequency ratio between the input 0 and input 1 received:

- Unbiased: 0 and 1 are inputted with the same frequency for both Bob<sub>1</sub> and Bob<sub>2</sub>

The CHSH values for Alice–Bob<sub>n</sub> are calculated by

$$I_{CHSH}^{(1)} = 2\sqrt{2}G, \quad I_{CHSH}^{(2)} = \sqrt{2}(1 + F). \quad (28)$$

Here, Bob<sub>1</sub> performs first measurement within intermediate strength while Alice and Bob<sub>2</sub> measure strongly. A comparison between the classical bound of  $I_{CHSH}$  values and the measured results is plotted in Figure 1b. As a result, we can see a Gaussian or optimal distributed pointer are both able to violate the Bell-CHSH inequality twice with tuned  $G$ , which is impossible to observe using a square pointer setting.

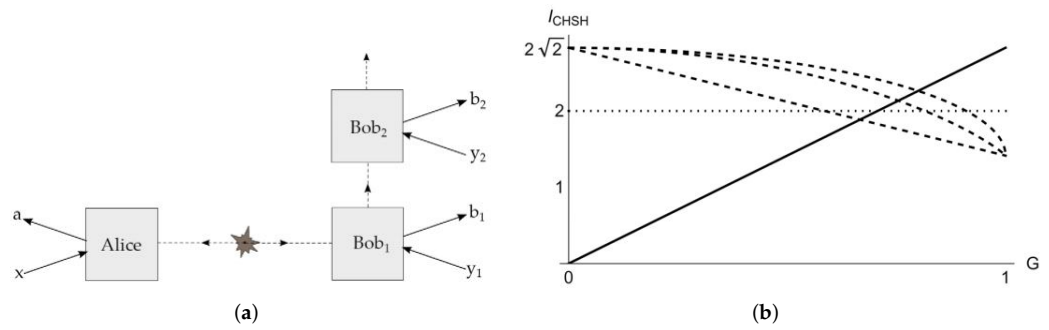


**Figure 1.** (a) A single Alice and several Bobs share nonlocality in Bell-CHSH scheme [34]. (b) (Solid)  $I_{CHSH}^{(1)}$  is plotted as a function of  $G$ , the measurement precision of Bob<sub>1</sub>. (Dashed)  $I_{CHSH}^{(2)}$  varies with  $G$  for optimal, Gaussian, and square pointer (from the top down) [34].

- Biased: 0 and 1 are inputted with different frequencies for all Bobs

In this case, we design a biased measurement protocol to investigate the limit for Bob's number to violate the Bell-CHSH inequality, and the answer is *No*: as the input bias increases, the sequence of violated Bobs becomes longer. Specifically, for the above measurement scheme where the 0/1 input frequency ratio approaches infinity, the  $n$ -th maximum violation of the inequality  $V_n = I_{CHSH}^{(n)} - 2$  decreases superexponentially with large values of  $n$

$$V_{n+1} \approx \frac{V_n^3}{4}. \quad (29)$$

This work brings the concept of weak measurements into Bell nonlocality theory for the first time, and explores the possibility for achieving multiple observer violations of the Bell-CHSH inequality under constraints of different trade-offs. However, although numerical evidence is used to demonstrate that it is impossible for an unbiased input Bob sequence to violate the classical CHSH bound twice, the concrete analytical proof still remains an open problem. Soon afterwards, Mal et al. [41] resolve the upper bound for Bell-CHSH violations analytically, using the formalism of a one-parameter class of POVMs [42,51,52]. It has been shown that the effect operator for weak measurements in the form of single parameter POVMs is described as

$$E^\lambda = (\mathbb{I} + \lambda n_i \sigma_i)/2, i = 1, 2, 3. \quad (30)$$

Here,  $\lambda \in (0, 1]$  represents the precision of measurements. We can also derive the relation between  $E^\lambda$  and sharp projectors  $P$  considering the white noise. For a two-energy-level system,  $E^\lambda$  is provided by

$$E^\lambda \equiv \{E_+^\lambda, E_-^\lambda | E_+^\lambda + E_-^\lambda = \mathbb{I}\}, \quad (31)$$

which satisfies

$$E_\pm^\lambda = \lambda P_\pm + \frac{1-\lambda}{2} \mathbb{I}. \quad (32)$$

The post-measurement state is now rewritten with the parameter  $\lambda$  as

$$\rho' = \sqrt{1-\lambda^2} \rho + (1-\sqrt{1-\lambda^2})(P_+ \rho P_+ + P_- \rho P_-), \quad (33)$$

and the probabilities to obtain the corresponding outcomes  $\pm$  are also calculated by

$$p(\pm) = \text{tr}[E_\pm^\lambda \rho] = \lambda \text{tr}[P_\pm \rho] + \frac{1-\lambda}{2}. \quad (34)$$

By comparing Equation (20) with Equation (33) and Equation (22) with Equation (34), we can easily obtain the transform between parameters of the above two formalisms:  $G = \lambda$ ,  $F = \sqrt{1 - \lambda^2}$ . Thus,  $\lambda$  describes the measurement precision for POVMs, while the optimal pointer setting is naturally derived:  $F^2 + G^2 = 1$ . That is to say, the weak or unsharp measurements described by a one-parameter class of POVMs are able to satisfy the optimal trade-off between information gain and disturbance for original states.

Next, we are going to discuss the upper bound of Bob's number for sharing Bell nonlocality with a single Alice. Following the work by Silva et al., we focus on a spin- $\frac{1}{2}$  entangled pair while Alice measures in the  $\hat{X}$  or  $\hat{Z}$  direction, and Bob's measure in the  $\frac{-(\hat{Z}+\hat{X})}{\sqrt{2}}$  or  $\frac{-\hat{Z}+\hat{X}}{\sqrt{2}}$  directions. In the above Bell-CHSH scenario,  $n - 1$  of Bob's must perform unsharp measurements, and the last Bob measures projectively. For Alice and the  $n$ -th Bob, the corresponding outcome  $a$  and  $b_n$  are obtained with the joint probability The

$$p(a, b_n) = p(a)p(b_n|a) = \frac{1}{2} \text{tr} \left[ \frac{\mathbb{I} + \lambda_n b_n \hat{y}_n \cdot \vec{\sigma}}{2} \rho_{n|y_1 \dots y_{n-1}} \right]. \quad (35)$$

Here, we use  $\rho_{n|y_1 \dots y_{n-1}}$  to denote the state after the measurements of Alice and Bob <sub>$n-1$</sub> , and the example for two Bob's to measure sequentially is described by the probability

$$p(a, b_2) = \frac{\sqrt{1 - \lambda_1^2}}{2} \frac{1 - ab_2 \lambda_2 \hat{y}_2 \cdot \hat{x}}{2} + \frac{1 - \sqrt{1 - \lambda_1^2}}{2} \frac{1 - ab_2 \lambda_2 \hat{x} \cdot \hat{y}_1 \hat{y}_1 \cdot \hat{y}_2}{2}, \quad (36)$$

the CHSH values are provided by  $I_{CHSH}^{(1)} = 2\sqrt{2}\lambda_1$  and  $I_{CHSH}^{(2)} = \sqrt{2}(1 + \sqrt{1 - \lambda_1^2})$ . A double violation is obtained when the first Bob keeps its precision  $\lambda_1$  in the range  $\in (1/\sqrt{2}, \sqrt{2}(\sqrt{2} - 1))$ . Next, we further increase the number of Bob's to 3, in which case the third Bob measures projectively while the first two Bob's both measure weakly. Thus, we calculate the joint probability as

$$\begin{aligned} p(a, b_3) = & \frac{1}{2} \left[ \sqrt{1 - \lambda_1^2} \sqrt{1 - \lambda_2^2} \frac{1 - ab_3 \lambda_3 \hat{y}_3 \cdot \hat{x}}{2} \right. \\ & + (1 - \sqrt{1 - \lambda_1^2}) \sqrt{1 - \lambda_2^2} \frac{1 - ab_3 \lambda_3 \hat{x} \cdot \hat{y}_1 \hat{y}_1 \cdot \hat{y}_3}{2} \\ & + \sqrt{1 - \lambda_1^2} (1 - \sqrt{1 - \lambda_2^2}) \frac{1 - ab_3 \lambda_3 \hat{x} \cdot \hat{y}_2 \hat{y}_2 \cdot \hat{y}_3}{2} \\ & \left. + (1 - \sqrt{1 - \lambda_1^2}) (1 - \sqrt{1 - \lambda_2^2}) \frac{1 - ab_3 \lambda_3 \hat{x} \cdot \hat{y}_1 \hat{y}_1 \cdot \hat{y}_2 \hat{y}_2 \cdot \hat{y}_3}{2} \right], \end{aligned} \quad (37)$$

where  $\lambda_2$  is, similarly, the measurement precision of the second Bob. After averaging over earlier inputs in all cases, we can obtain the CHSH value between Alice and the third Bob

$$I_{CHSH}^{(3)} = \frac{(1 + \sqrt{1 - \lambda_1^2})(1 + \sqrt{1 - \lambda_2^2})}{\sqrt{2}}. \quad (38)$$

It is required to use  $\lambda_1 > 1/\sqrt{2}$  and  $\lambda_2 > 2/(\sqrt{2} + 1)$  to achieve Bell-CHSH inequality violations for the first and second Bob; thus, we can obtain the upper bound for the CHSH value for the third Bob from Equation (38), which is impossible to be greater than 2.

In the above discussion, Bob's measurement settings conform to orthogonality by default, and next Mal et al. further consider the more general POVM operators, relaxing the orthogonality constraint. In this case, we can rewrite the measurement directions for Bob <sub>$n$</sub>  as

$$\begin{aligned} y_n^0 &= \cos \theta_{n0} \hat{Z} + \sin \theta_{n0} \hat{X} \\ y_n^1 &= \cos \theta_{n1} \hat{Z} + \sin \theta_{n1} \hat{X}, \end{aligned} \quad (39)$$

which remain unchanged for Alice ( $\hat{X}$  or  $\hat{Z}$ ). With the nonorthogonal measurement settings defined above, we calculate the violations for three Bobs and find that it is impossible for more than two Bobs to share Bell-CHSH nonlocality with Alice, even if we introduce more variables in the measurement settings. In particular, the above paper shows that those entangled Alice–Bob pairs are not special, which means Bobs can be selected from (Bob<sub>1</sub>, Bob<sub>2</sub>), (Bob<sub>1</sub>, Bob<sub>3</sub>), and (Bob<sub>2</sub>, Bob<sub>3</sub>) with different unsharpness parameters, respectively.

At present, the research on multi-party sharing of quantum correlation based on sequence measurement mainly focuses on quantum entanglement, EPR steering, and Bell nonlocality. Among them, EPR steering describes the nonclassical phenomenon for a pair of entangled qubits, where one side can apply local measurements to change the state of the other side. EPR steering has a natural asymmetry and is considered to be a necessary resource for one-sided device-independent quantum information processing [4]. For these levels of quantum correlations, as explained in Section 1, the constraint requirements are successively enhanced from quantum entanglement, EPR steering, and to Bell nonlocality (Figure 2a), while the corresponding sequential measurement scenarios are described in the next section.

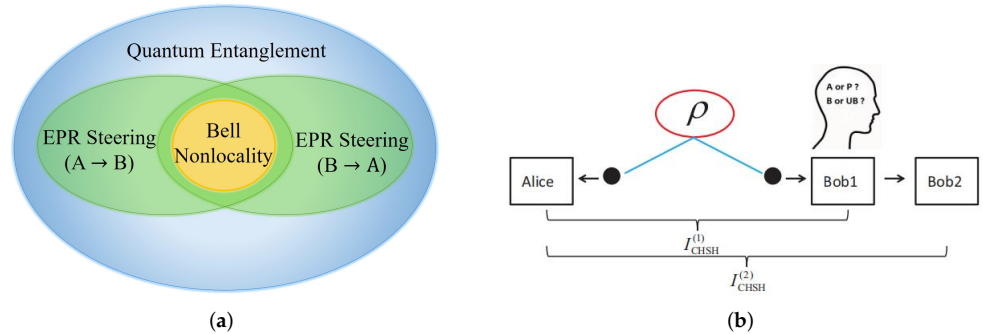


**Figure 2.** (a) Illustration of quantum correlation hierarchy. (b) A scenario of entangled states to achieve nonlocality sharing in sequential measurement, divided into active (“A”) and passive (“P”) cases by carefully examining the motivation of Bob<sub>1</sub>, where “B” and “UB” represent biased and unbiased input settings [53].

#### 4. Advances in Sequential Unsharp Measurements for Quantum Correlation Recycling

##### 4.1. Theoretical Exploration in Quantum Mechanics Foundation

In 2018, Bera et al. [54] characterized quantum entanglement from the entanglement witness [7,55–58], which is provided by a Hermitian operator and substituted with the parameter  $\lambda$  corresponding to the POVM form. Thus, for the state  $|\psi^+\rangle\langle\psi^+| = \frac{1}{\sqrt{2}}(|01\rangle + |10\rangle)$ , the effective entanglement witness is written as

$$W_0^\lambda = \frac{1}{4}(\mathbb{I} \otimes \mathbb{I} + \sigma_z \otimes \lambda\sigma_z - \sigma_x \otimes \lambda\sigma_x - \sigma_y \otimes \lambda\sigma_y). \quad (40)$$

For all separable states  $\rho_s$  from Alice–Bob pairs, the expectation value after witness detection is calculated by

$$\begin{aligned} \text{tr}(W_0^\lambda \rho_s) &= \text{tr}[(\lambda W_0 + \frac{1}{4}(1 - \lambda)\mathbb{I} \otimes \mathbb{I})\rho_s] \geq 0 \\ W_0 &= \frac{1}{4}(\mathbb{I} \otimes \mathbb{I} + \sigma_z \otimes \sigma_z - \sigma_x \otimes \sigma_x - \sigma_y \otimes \sigma_y). \end{aligned} \quad (41)$$

The negative measured values of a witness demonstrate the nontrivial lower bound for entanglement measures [59], which requires weaker quantum correlation than the Bell inequality [60,61]. For the entangled state shared between Alice and Bob, the measurement process is of the form

$$\text{tr}[\rho(P_{\hat{n}}^i \otimes E_{j|\hat{m}}^{\lambda})], \quad (42)$$

where  $P_{\hat{n}}^i$  corresponds to the projective measurement by Alice, and  $E_{j|\hat{m}}^{\lambda}$  is an effective operator in the POVM form for weak measurements performed by Bobs.

For the maximally entangled state  $|\psi^+\rangle\langle\psi^+|$ , there are up to 12 Bobs that can detect entanglement with one Alice through witness evidences (higher than the 2 represented by the Bell inequality) under arbitrary and possibly unequal sharpness parameters (i.e.,  $\lambda_1 < \lambda_2 < \dots < \lambda_n$ ). It is also found that the number of Bobs is positively correlated with the entanglement degree of the initial nonmaximally entangled quantum pure state, which provides a rough but operable measure of entanglement.

In the field of EPR steering, Sasinal et al. [62] investigate an upper bound on the number of Bobs to steer a single Alice analogous to the Bell-CHSH inequality. They propose the Cavalcanti–Foster–Fuwa–Wiseman (CFFW) inequality [63] to detect steering from Bob to Alice, of which Alice performs two unbiased dichotomic measurements  $A_1, A_2$  and Bob performs  $B_1, B_2$ . The inequality is provided by

$$S_{BA} = \sqrt{\langle (B_1 + B_2)A_1 \rangle^2 + \langle (B_1 + B_2)A_2 \rangle^2} + \sqrt{\langle (B_1 - B_2)A_1 \rangle^2 + \langle (B_1 - B_2)A_2 \rangle^2} \leq 2. \quad (43)$$

Similarly, a series of steering inequalities is constructed assuming that both sides of an entangled pair are allowed to perform  $n$  dichotomic measurements on their respective subsystems, and the mathematical form is as follows

$$F^n = \frac{1}{\sqrt{n}} \left| \sum_{i=1}^n \langle A_i \otimes B_i \rangle \right| \leq 1. \quad (44)$$

Here,  $A_i = \hat{u}_i \cdot \vec{\sigma}$ ,  $B_i = \hat{v}_i \cdot \vec{\sigma}$ ,  $\vec{\sigma} = (\sigma_x, \sigma_y, \sigma_z)$ ,  $\hat{u}_i$  are unit vectors and  $\hat{v}_i$  are orthonormal for  $n = 2$  or  $3$ . The above inequality is called the Cavalcanti–Jones–Wiseman–Reid (CJWR) inequality [64]. They study the preservation of quantum steering after multiple sequential measurements and find that, when all observers take dichotomous measurements, two Bobs can achieve steering over Alice simultaneously, beyond the monogamy relation limit. Furthermore, when increasing the number of measurement basis settings, the steering from three Bobs to Alice can be achieved through 3-setting CJWR inequality. Thus, they conclude that there are at most  $n$  Bobs that can prove EPR steering with one Alice using the  $n$ –setting CJWR inequality. Subsequently, the work by Shenoy H. et al. [65] shows that, in an isotropic entangled state of local dimension  $d$ , there are  $N \sim d/\log d$  number of Bobs that can steer single Alice, indicating that an arbitrarily large number of continuous EPR steering is able to be realized with independent and unbiased inputs. In addition, they prove that the above conclusion also applies in cases where each Bob does not know its position in the sequence. Recently, a study [66] investigating the sharing of EPR steering by two-sided sequences shows that, for the initial shared state of a two-qubit entangled pure state, there are unbounded measurement sequences from both sides that can generate EPR steering between multiple independent observers. This conclusion also applies to a specific class of mixed entangled states.

Quantum nonlocality multi-observer sharing under sequential weak measurements is mainly focused on the violations of Bell-CHSH inequality and its derived forms. In 2019, Das et al. [35] successively increased the number  $n$  of measurement settings per observer to study the nonlocality sharing among multiple Bobs and a single Alice. In practice, they use the derivative forms of the Bell-CHSH inequality to deal with arbitrary number

of dichotomic measurements, taking the chained three and four settings of Bell-CHSH inequality [48,67,68] as an example; the mathematical form is expressed as follows

$$\begin{aligned} \text{chain}^3 &= |\langle A_1 B_1 \rangle + \langle A_2 B_1 \rangle + \langle A_2 B_2 \rangle \\ &\quad + \langle A_3 B_2 \rangle + \langle A_3 B_3 \rangle - \langle A_1 B_3 \rangle| \leq 4, \\ \text{chain}^4 &= |\langle A_1 B_1 \rangle + \langle A_2 B_1 \rangle + \langle A_2 B_2 \rangle + \langle A_3 B_2 \rangle \\ &\quad + \langle A_3 B_3 \rangle + \langle A_4 B_3 \rangle + \langle A_4 B_4 \rangle - \langle A_1 B_4 \rangle| \leq 6. \end{aligned} \quad (45)$$

Here,  $A_1, A_2, A_3, A_4$  and  $B_1, B_2, B_3, B_4$  denote the dichotomic measurement settings within different inequalities for Alice and Bob, respectively. In addition, there are many other forms of  $n$ -setting Bell-CHSH inequality, such as three-setting Gisin inequality [69] and the  $I_{3322}$  inequality [70] derived by Collins et al., and four-setting Gisin inequality [69], DZC (Deng–Zhou–Chen) inequality [71], BG (Brunner–Gisin) inequality [72], and the first and second AIIG (Avis–Imai–Ito–Gisin) inequalities [73,74]. The results show that, when the entangled pair performs three or four dichotomic measurements, the number of Bobs that can share nonlocality with one Alice does not increase; in other words, there are still no more than two (unlike in the case of EPR steering), and this result can be extrapolated to the  $n$ -settings case. Using these inequalities, they further investigate nonlocality sharing in nonmaximally entangled pure states, where any two-particle pure state can be written in the form of Schmidt decomposition [48,75].

$$|\psi(\alpha)\rangle = \cos \alpha |00\rangle + \sin \alpha |11\rangle. \quad (46)$$

The parameter  $\alpha$  satisfies  $0 \leq \alpha \leq \frac{\pi}{2}$  and describes the maximum entangled pure state with the value  $\frac{\pi}{4}$ . They calculate the minimum  $C$  ( $C = \sin 2\alpha$  [76]) that holds the double violation of Bobs with a single Alice using the above local realist inequalities. The result shows that, when the initial state is nonmaximally entangled pure state, the sharing of Bell nonlocality among multiple Bobs and one Alice is the most robust for CHSH inequality, which is also observed in the case of mixed states.

The work by Ren et al. [53] provides an in-depth analysis for two types of nonlocality sharing via weak measurements. Based on whether Bob<sub>1</sub> has the conscious thought for sharing nonlocality to Bob<sub>2</sub>, that is, whether there is the motivation for Bob<sub>1</sub> to help Bob<sub>2</sub> achieve the maximum CHSH inequality violation, nonlocality sharing is divided into active and passive cases. In particular, active nonlocality sharing has never been mentioned in previous studies, and there are many counterintuitive results extremely different from the passive one. It is found that these two sharing scenarios (Figure 2b) are distinct under sequential measurement: in active nonlocality sharing, the measurement sharpness performed by Bob<sub>1</sub> is not limited except for the ideal strong measurement (which completely destroys the quantum entanglement). Even if Bob<sub>1</sub> is weakly measured using a square pointer rather than an optimal pointer, a double violation of the CHSH inequality can still be observed, which is impossible for passive nonlocality sharing. These results undoubtedly shed new light on the interaction between Bell nonlocality and quantum measurements.

Furthermore, Saha et al. [77] consider the case of nonlocality sharing in the tripartite scenario and study it from the two aspects of standard tripartite nonlocality [78] and genuine tripartite nonlocality [79]. The standard tripartite nonlocality detection is implemented by a violation of the Mermin inequality (derived from Bell-type inequality) [78] and written as follows

$$M = |\langle A_2 B_1 C_1 \rangle + \langle A_1 B_2 C_1 \rangle + \langle A_1 B_1 C_2 \rangle - \langle A_2 B_2 C_2 \rangle| \leq 2, \quad (47)$$

where Alice, Bob, and Charlie perform two dichotomic measurements  $\{A_x, B_y, C_z, x, y, z \in \{1, 2\}\}$ , respectively. For quantum mechanics, the maximum violation value of the Mermin inequality is 4, which is achieved within the three-qubit GHZ state [80]

$$|\psi_{GHZ}\rangle = \frac{1}{\sqrt{2}}(|000\rangle + |111\rangle). \quad (48)$$

Nevertheless, the violation of Mermin inequality does not represent genuine tripartite nonlocality, which means that quantum nonlocality can be observed in any possible partitions of the tripartite state [79,81]. This strongest form is characterized by the Svetlichny inequality [79], which is mathematically provided as

$$S = |\langle A_1 B_1 C_1 \rangle + \langle A_2 B_1 C_1 \rangle - \langle A_1 B_2 C_1 \rangle + \langle A_2 B_2 C_1 \rangle + \langle A_1 B_1 C_2 \rangle - \langle A_2 B_1 C_2 \rangle + \langle A_1 B_2 C_2 \rangle + \langle A_2 B_2 C_2 \rangle| \leq 4. \quad (49)$$

The maximum quantum violation in this situation is  $4\sqrt{2}$ . They set up a scenario similar to that of the bipartite one, where three particles of spin- $\frac{1}{2}$  share an entangled state and are spatially separated from each other. Alice and Bob perform measurements on the first and second particles, respectively, and multiple Charlies perform sequential weak measurements on the third particle. The results demonstrate that, in the case of sequential measurement scheme, the standard tripartite nonlocality is able to have more observers than the genuine tripartite nonlocality, that is, at most six, and two Charlies can simultaneously prove the corresponding tripartite nonlocality with a single Alice and a single Bob. This interesting result also illustrates the concept that two tripartite nonlocalities are not equivalent in the context of quantum correlation sharing. In a similar work later, Maity et al. [82] employ the witness operator of genuine tripartite entanglement [7,83–85] rather than entanglement inequalities. By abandoning the requirement of device independence for the inequality test, the number of Charlies that can share genuine tripartite entanglement for the GHZ state is increased to 12. This is of great significance for the recycling of genuine multipartite entanglement resources in various quantum information processing tasks [20,86–90].

For the single-particle quantum system, we pay more attention to another important property, namely quantum contextuality. Noncontextuality is an intuitive feature of classical systems; however, Kochen and Specker propose that classical noncontextuality is in conflict with quantum mechanics, which is known as the Kochen–Specker (KS) theorem [11]. The relationship between contextuality and nonlocality of quantum physics lies in the fact that local hidden variable theory is a special type of noncontextual hidden variable theory [91], and some proofs of KS theorem can also be converted into logical proofs of Bell theorem [80,92]. Kumari et al. [93] investigate the multi-observer sharing of nonlocality and nontrivial preparation contextuality by violating Bell’s local realist inequalities. Considering that Alice and Bob set the number of dichotomic measurements to  $2^{n-1}$  and  $n$ , they write the family of Bell expressions as

$$\mathcal{B}_n = \sum_{y=1}^n \sum_{i=1}^{2^{n-1}} (-1)^{x_y^i} A_{n,i} \otimes B_{n,y}, \quad (50)$$

where  $x_y^i$  is the  $y$ th bit of Alice’s  $n$ -bit input string  $x^i$  used in implementation for an  $n$ -bit parity-oblivious multiplexing (POM) game, which aims to achieve the preparation noncontextual assumptions. When  $n = 2$ , the above  $\mathcal{B}_n$  becomes the CHSH expression. The local and nontrivial preparation noncontextuality upper bounds are

$$\begin{aligned} (\mathcal{B}_n)_{local} &\leq n \binom{n-1}{\lfloor \frac{n-1}{2} \rfloor}, \\ (\mathcal{B}_n)_{pnc} &\leq 2^{n-1}. \end{aligned} \quad (51)$$

It can be seen that, when  $n > 2$ ,  $(\mathcal{B}_n)_{pnc} < (\mathcal{B}_n)_{local}$ . This suggests that nontrivial preparation contextuality is a weaker form of quantum correlations that may also exist in local models, so it is easier to achieve multi-observer sharing than that of nonlocality. Their

results validate this point of view with numerical solutions, where an arbitrary number of Bobs can demonstrate a violation of nontrivial preparation noncontextuality under sequential weak measurements, even if the measurement setting is chosen to be unbiased.

In 2020, Brown et al. [94] proposed a new idea to break the limit on Bob's number in sequential nonlocality sharing. They note that there is an implicit assumption within the previous study in which each Bob sets up the equal sharpness for its two dichotomic measurements. Their new scheme takes into account the most general measurement strategy, employing measurement settings with unequal sharpness. Similarly, they define POVM operators for Alice and  $n$  Bobs:

$$\begin{aligned} A_{0|0} &:= \frac{1}{2}(\mathbb{I} + \cos(\theta)\sigma_z + \sin(\theta)\sigma_x), \\ A_{0|1} &:= \frac{1}{2}(\mathbb{I} + \cos(\theta)\sigma_z - \sin(\theta)\sigma_x); \\ B_{0|0}^{(k)} &:= \frac{1}{2}(\mathbb{I} + \sigma_z), \\ B_{0|1}^{(k)} &:= \frac{1}{2}(\mathbb{I} + \gamma_k\sigma_x). \end{aligned} \quad (52)$$

Here,  $A(B)_{b|y}$  is the POVM operator for the measurement outcome  $b$  with input  $y$ ,  $\theta \in (0, \frac{\pi}{4}]$ , and  $k = 1, 2, \dots, n$ , which corresponds to the indexes of multiple Bobs.  $\gamma_k$  is the measurement sharpness parameter for each Bob, where  $\gamma_k = 1$  means an ideal projective (sharp) measurement, and  $\gamma_k = 0$  does not cause any disturbance to the quantum state. In practice, they design an appropriate measurement strategy, which defines that  $\varepsilon > 0$ ,  $\gamma_1(\theta) = (1 + \varepsilon)(1 - \cos(\theta)) / \sin(\theta)$ , and then the recursive relation for  $\gamma_k$  ( $k > 1$ ) is provided as

$$\gamma_k(\theta) = \begin{cases} (1 + \varepsilon) \frac{2^{k-1} - \cos(\theta)P_k}{\sin(\theta)} & \text{if } \gamma_{k-1}(\theta) \in (0, 1) \\ \infty & \text{otherwise} \end{cases}. \quad (53)$$

Here,  $P_k = \prod_{j=1}^{k-1} (1 + \sqrt{1 - \gamma_j^2(\theta)})$ , and, if the expected CHSH value  $I_{CHSH}^{(k)}$  is less than the classical bound ( $= 2$ ), then  $\gamma_k(\theta) = \infty$ .

Using the above strategy, they can define  $n$  valid sharpness parameters  $\gamma$  sequentially using applicable  $\theta$  within the specified range, and then each Bob can achieve the expected  $I_{CHSH}$  value beyond the classical bound. The numerical result shows that arbitrarily many independent Bobs can achieve Bell-CHSH nonlocality sequential sharing with a single Alice (Figure 3a). They also discuss the requirement for  $\theta$  and find that this value rapidly decreases double-exponentially as the number of Bob  $n$  increases. Later on, the work of Zhang et al. [95] extends the above conclusion to the higher dimensional case, verifying the unbounded sharing of a single bipartite entangled state in any dimension rather than just a two-qubit entangled state. They also discuss the genuine tripartite nonlocality sharing following the updated measurement strategy by Brown et al. For the generalized GHZ state  $|\psi_\alpha\rangle = \cos \alpha |000\rangle + \sin \alpha |111\rangle$ , through violations of the Svetlichny inequality [79], it is found that no more than two Charlies can share genuine nonlocality with one Alice and one Bob.

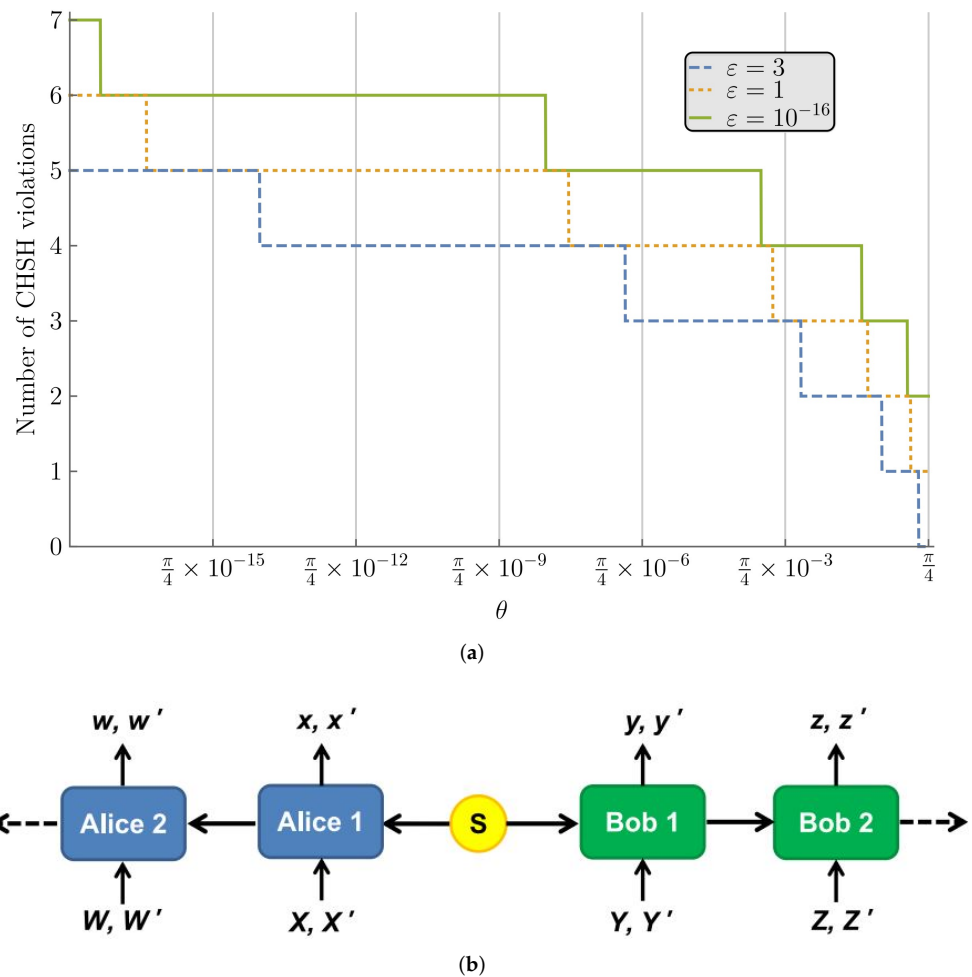


**Figure 3.** (a) The maximum number  $n$  of Bobs that can simultaneously violate the Bell-CHSH inequality using the updated measurement strategy as a function of  $\theta$ . These numerical results take into account different values of  $\varepsilon$  to satisfy  $\gamma_k(\theta) < 1$  and likewise show that  $\theta$  decreases faster exponentially as the number  $n$  increases [94]. (b) Multi-observer Bell nonlocality sharing in two-sided sequential measurements [96].

The number of two-sided nonlocality recycling is also an open and interesting question when considering multiple Alice–Bob measurement scenarios. In 2021, Cheng et al. [96] considered that two qubits are simultaneously recycled by multiple observers on both sides, achieving Bell nonlocality sequential sharing (Figure 3b). Their measurement assumptions are the same as those of Brown et al. [94], but the results are quite opposite. They present strong analytical and numerical evidence that Bell nonlocality cannot be shared simultaneously between multiple observers on two sides (Alices and Bobs). This restriction on recycling qubits can be viewed as a type of one-sided monogamous relationship for Bell nonlocality sharing. The more detailed analyses and corresponding semi-analytical results are published in a companion paper [97], and they argue that, if more measurements of higher-dimensional quantum systems (multi-qubit entangled states) can be allowed, then each pair of Alices and Bobs has the potential to share Bell nonlocality arbitrarily. This conjecture is later developed by Chirag et al. [98], who investigate the sequential detection of genuine multipartite entanglement (GME) of the shared state. They set the initial state to an  $N$ -partite GHZ state, shared among  $N$  space-separated parties, i.e., Alices, Bobs, Charlies, . . . . Their strategy is to detect genuine multipartite entanglement in turn by recycling any fixed subset of all qubits to form a hierarchical measurement scenario. The results show that, in such a measurement hierarchy, each partite performs sequential genuine multipartite entanglement detections on the corresponding qubit, leading to an unbounded

sequence. It is worth noting that, although the current measurement scheme cannot realize the sharing of Bell-CHSH nonlocality from both sides for two-qubit entangled states [96], the recycling sequence for pairs of observers to reach entanglement witnessing can be arbitrarily long for any pure entangled two-qubit state initially [99]. This finding can be seen as strong evidence for a clear distinction between “entanglement nonlocality” and “Bell nonlocality”, which have similar performance [94,100] in the context of one-sided multi-observer sharing.

In addition to the conceptual appeal of fundamental physics, the recycling of quantum correlations has also been studied in the extraction of quantum randomness. Random numbers play an important role in science and engineering as an essential resource for cryptography [101], scientific simulations [102], and fundamental physics tests [2]. The intrinsic unpredictability of quantum mechanics gives it a natural advantage over deterministic classical physics in describing true randomness [36–38]. Specifically, the device-independent certification of randomness [38] can be achieved by violations of Bell inequality with the measured output on the entangled state.

In 2017, Curchod et al. [103] combined this scheme with a sequential weak measurement scenario to overcome the limited amount of randomness that previous projective measurements could certify in an entangled pair. In the previous study [104,105], it is shown that, for  $d$ -dimensional particles sharing entangled states, at most  $2 \log_2 d$  bits of randomness can be certified on either side with a single measurement. In the weak measurement scenario, the quantum state after measurement retains a certain degree of entanglement and can still be used as a subsequent randomness source. Based on this, their proposed scheme performs sequentially weak measurements with  $n$  Bobs and constructs a corresponding exponentially increasing number ( $\sum_{i=1}^n 2^i = 2(2^n - 1)$ ) of measurement choices for  $n$  measurements by a single Alice. They use *min entropy* to quantify the number of random bits and find that the  $n$ -Bob sequence can be extracted for  $m$  random bits ( $n > m$ ) with the appropriate parameter selection, which means that the above random source is potentially unbounded. However, their work put no control for the robustness of noise into effect, and this shortcoming is remedied in later studies [106], which also migrates to the one-sided device-independent sequential measurement scenario. In 2020, Bowles et al. [107] used the NPA hierarchy [108,109] as an effective tool to investigate randomness certification bounding sets utilizing the measurement sequence. They introduce noise parameter  $\eta$  into the two-qubit entangled state

$$\rho(\eta) = (1 - \eta) \left[ \frac{(|00\rangle + |11\rangle)}{\sqrt{2}} \right] + \eta \mathbb{I}/4, \quad (54)$$

and set up one Alice and two Bobs to perform the one-sided sequential measurement. The results show that more than 2.3 bits of local randomness can be reliably certified, exceeding the theoretical maximum (2 bits) in the nonsequential measurement scheme. The numerical results also indicate that, at the noise level approaching 4 %, an advantage of sequential strategy in generating randomness can be observed, which is of great significance in guiding relevant experiments.

#### 4.2. Experimental Demonstration Based on Optical Qubits

At present, the experimental verification of quantum correlation multi-observer sharing mainly relies on optical systems. In 2017, Schiavon et al. [110] built a theoretical model of a two-photon state with maximum polarization entanglement, designing and demonstrating the corresponding experiments to achieve a double violation of the Bell-CHSH inequality under sequential weak measurements. Their theoretical model follows Silva et al. [34], with three observers represented by Alice, Bob<sub>1</sub>, and Bob<sub>2</sub>, respectively, while the weak measurement scheme requires an ancillary qubit system. They use the ancilla to

achieve a controllable strength entanglement with the measured system, and then perform a strong readout on the ancillary qubit. For  $\text{Bob}_1$ , a controlled phase gate

$$CP_\varepsilon = |H\rangle\langle H| \otimes \mathbb{I} + |V\rangle\langle V| \otimes e^{i\varepsilon\sigma_z} \quad (55)$$

is used to establish the entanglement between the ancilla and Bob's side qubit. The ancilla system is first prepared in the state  $|+\rangle$  and then measured in the  $\{|+\rangle, |-\rangle\}$  basis after the gate operation. Thus, they can control the measurement strength by adjusting the amount of gate rotation parameter  $\varepsilon$  to measure the particle in the  $\{|H\rangle, |V\rangle\}$  basis, while a strong projective measurement is performed with  $\varepsilon = \pi/2$ . More generally, to perform the measurement on an arbitrary basis  $\{|\omega_{y_1}\rangle, |\omega_{y_1}^\perp\rangle\}$ , they should use a rotation operator  $R_{y_1}$  satisfying

$$R_{y_1}|\omega_{y_1}\rangle = |H\rangle, R_{y_1}|\omega_{y_1}^\perp\rangle = |V\rangle. \quad (56)$$

The entangled two particles share a singlet state

$$|\Psi^-\rangle = \frac{|H\rangle|V\rangle - |V\rangle|H\rangle}{\sqrt{2}}, \quad (57)$$

where one Alice and two Bobs perform measurements on its side. Alice selects from the measurement choice  $x \in \{0, 1\}$ , measures the system projectively, and obtains the result  $a \in \{+, -\}$ . On Bob's side, the observed state collapses into  $|\psi_{a|x}\rangle$ , and the joint system with the ancillary qubit  $|\psi_{a|x}\rangle \otimes |+\rangle$  is rotated into  $(\alpha|H\rangle + \beta|V\rangle)|+\rangle$ , where  $\alpha = \langle\omega_{y_1}|\psi_{a|x}\rangle$  and  $\beta = \langle\omega_{y_1}^\perp|\psi_{a|x}\rangle$ . Then, they use the controlled phase gate (parameter  $\varepsilon$ ) to transform the ancillary state while the system qubit is  $|V\rangle$ , and the joint state becomes

$$(\alpha|H\rangle + \beta|V\rangle)|+\rangle \rightarrow \alpha|H\rangle|+\rangle + \beta|V\rangle(\cos\varepsilon|+\rangle + i\sin\varepsilon|-\rangle). \quad (58)$$

The last step is to rotate the state back to the measurement basis of  $\text{Bob}_1$  inversely by  $R_{y_1}^\dagger$ ; after that, the state is provided by

$$\alpha|\omega_{y_1}\rangle|+\rangle + \beta|\omega_{y_1}^\perp\rangle(\cos\varepsilon|+\rangle + i\sin\varepsilon|-\rangle). \quad (59)$$

In the sequential measurement scheme,  $\text{Bob}_1$  performs the measurement on the second qubit in the basis  $\{|+\rangle, |-\rangle\}$ , and  $\text{Bob}_2$  measures the first qubit in the basis  $\{|\nu_{y_2}\rangle, |\nu_{y_2}^\perp\rangle\}$  projectively, according to the input  $y_2 \in \{0, 1\}$ . When Alice measures in the directions  $-\frac{(Z+X)}{\sqrt{2}}$  or  $\frac{(-Z+X)}{\sqrt{2}}$  and Bob measures in the direction  $Z$  or  $X$ , they can obtain the predictive CHSH value with the parameter  $\varepsilon$

$$I_{\text{CHSH}}^{(1)} = 2\sqrt{2}\sin^2\varepsilon, \quad I_{\text{CHSH}}^{(2)} = \sqrt{2}(1 + \cos\varepsilon). \quad (60)$$

Experimentally, they utilize the optical setup (Figure 4) to verify the above theoretical model. The entangled photon pairs are collected from a periodically poled potassium titanyl phosphate (PPKTP) crystal in a polarization-based Sagnac interferometer [111] and sent to the Alice and Bob sides. Alice and  $\text{Bob}_2$  implement a projective measurement scheme including an HWP (HWP1 and HWP6) and a PBS to obtain the polarization information, while  $\text{Bob}_1$  designs a receiving apparatus for the weak measurement. The photons go through  $\text{Bob}_1$ 's apparatus and then reach  $\text{Bob}_2$ , where HWP2 and HWP5 are employed to achieve polarization rotation  $R$  and  $R^\dagger$ . Inside the Sagnac interferometer, they use HWP3 and HWP4 as phase retarders within spatially separated clockwise and anticlockwise paths, which correspond to the ancillary qubit. For an input pure state on Bob's side

$$|\psi_{in}\rangle = \alpha|\omega_{y_1}\rangle + \beta|\omega_{y_1}^\perp\rangle, \quad (61)$$

the output state is transformed into

$$|\psi_{out}\rangle = \alpha|\omega_{y_1}\rangle|2\rangle + \beta|\omega_{y_1}^\perp\rangle(\cos \varepsilon|2\rangle + \sin \varepsilon|3\rangle), \quad (62)$$

of which  $|2\rangle$  and  $|3\rangle$  correspond to the two output ports of the Sagnac interferometer, and also represent the measurement basis  $\{|+\rangle, |-\rangle\}$ . They plot the  $I_{CHSH}^{(1)}$  and  $I_{CHSH}^{(2)}$  measured with the parameter  $\varepsilon$  varying from 0 to  $\frac{\pi}{2}$  in Figure 5a, and the experimental results show a high agreement with the theoretical model. It is demonstrated by the experimental evidence that the double violation of CHSH inequalities is achieved, and hence Bell nonlocality can be shared between three observers (Alice–Bob<sub>1</sub> and Alice–Bob<sub>2</sub>) using two-photon maximally entangled state. A similar work [112] is proposed by Hu et al. and realizes optimal weak measurements by employing the path degree of freedom of photons as the pointer. Note that, in practice, they both use the Bob<sub>2</sub> part to detect the output value of Bob<sub>1</sub> because the weak measurement of Bob<sub>1</sub> is achieved by coupling the photons' polarization to two separated paths, and then outcomes are encoded in the path information after the measurement.

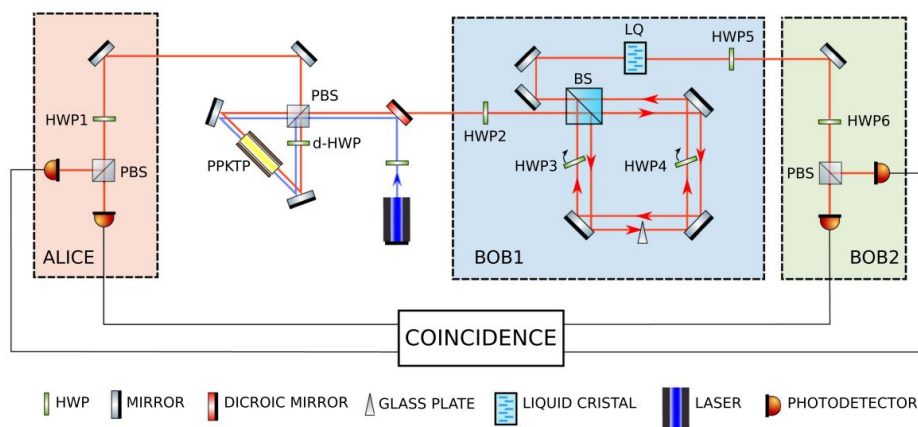


**Figure 4.** The demonstration of the optical experimental setup [110].

The experimental demonstration of multiple-observer quantum EPR steering is exploited both in one-sided and two-sided sequential weak measurement schemes. In 2020, Choi et al. [113] investigated violations of the linear EPR steering inequality in the form of Equation (43) [64] by a single Alice and three Bobs, with the number of measurement settings  $i = 3$ . They use a beta-barium borate (BBO) crystal under type-II spontaneous parametric down-conversion (SPDC) process [114] to produce entangled photon pairs, and the initial state is the singlet state, maximally entangled. In the experimental setup, Bob<sub>1</sub> and Bob<sub>2</sub> employ a half-wave plate to adjust the measurement strength  $\lambda_1$  and  $\lambda_2$ , while Bob<sub>3</sub> performs the projective measurement. The steering parameters of Alice–Bob<sub>1</sub>, Alice–Bob<sub>2</sub>, and Alice–Bob<sub>3</sub> are obtained simultaneously from the joint measurement probability, that is, experimentally measured and normalized data between two detectors in the end. As a result, they observe the quantum correlations sharing between four parties and the triple violations of EPR steering inequality setting  $\lambda_1 = 0.64$  and  $\lambda_2 = 0.76$ , with more than 40 standard deviations. The other EPR steering sharing among multiple observers in the two-sided scheme is explored by Zhu et al. [115] later, and they experimentally achieve quantum correlations sharing with two Alices and two Bobs. Specifically, it is shown that double EPR steering is realizable between two pairs of Alice–Bob (Alice<sub>1</sub>–Bob<sub>1</sub>/Alice<sub>2</sub>–Bob<sub>2</sub>) under two-sided sequential weak measurements when Alice<sub>1</sub> and Bob<sub>1</sub> measure with equal strength, which cannot be achieved in the Bell-CHSH scenario. It needs to be emphasized that, in the one-sided case, multiple Bobs are required to realize the steering of a single Alice with the same measurement settings, while, in the two-sided steering case, the target of Bobs is to steer the corresponding Alices, the measurement settings choice of which is mutually independent.

Anwer et al. [116] theoretically prove that an arbitrary number of observers can share nonclassicality via preparation contextuality, which is robust even in the existence of realistic white noise. In the following experiment, they demonstrate sequential weak measurements for a single photon within shifted Sagnac interferometers, while Alice randomly chooses the preparation state, which is then reaching Bob<sub>1</sub>, passing to Bob<sub>2</sub>, and ending at Bob<sub>3</sub>. Here, Bob<sub>1</sub> and Bob<sub>2</sub> perform weak measurements, while Bob<sub>3</sub> measures projectively. They test three preparation noncontextuality inequalities for Alice–Bob<sub>1</sub>, Alice–Bob<sub>2</sub>, and Alice–Bob<sub>3</sub>, and the experimental data show that all these pairs can violate inequalities and share preparation contextuality without requiring entanglement.

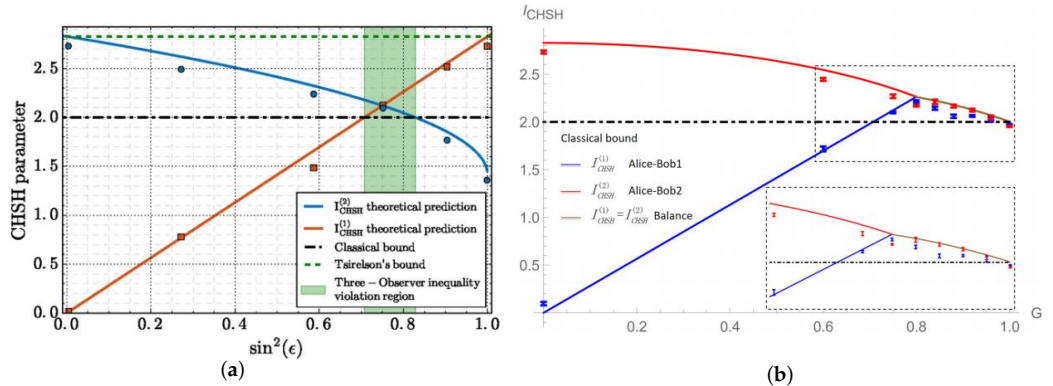


**Figure 5.** (a) Experimental results of  $I_{CHSH}^{(1)}$  (red squares) and  $I_{CHSH}^{(2)}$  (blue circles) with the values of  $\epsilon$  varying. The corresponding solid lines demonstrate their expected values. In particular, the  $\epsilon$ -value region that implements the double CHSH violation is highlighted in green [110]. (b) The experimental report for Bell nonlocality sharing via not-so-weak measurements. The brown curve is calculated by the theoretical model for  $G > 0.8$  and  $I_{CHSH}^{(1)} = I_{CHSH}^{(2)}$  in that situation. The red and blue dots represent experimental results for  $I_{CHSH}^{(2)}$  and  $I_{CHSH}^{(1)}$  and show good agreement with model predictions [117].

The 2020 work by Feng et al. [117] improves the measurement protocol to achieve nonlocality sharing with near-maximum strength, that is, not-so-weak measurements. They point out that the original scheme from Silva et al. [34] only takes the maximization of  $I_{CHSH}^{(1)}$  into consideration for the measurement directions selection of Bob<sub>1</sub>, which comes at the expense of lowering the upper bound of  $I_{CHSH}^{(2)}$  [53]. A more appropriate choice to achieve the double Bell-CHSH violation with wider range of the measurement strength falls on maximizing the min value between  $I_{CHSH}^{(1)}$  and  $I_{CHSH}^{(2)}$ , rather than  $I_{CHSH}^{(1)}$  or  $I_{CHSH}^{(2)}$  separately. Their scheme can be demonstrated as follows, Alice measures in the directions Z or X while the measurement directions for Bob depend on the value of precision G:

- if  $G \leq 0.8$ , the maximization of  $\min(I_{CHSH}^{(1)}, I_{CHSH}^{(2)})$  is equivalent to maximize the value of  $I_{CHSH}^{(1)}$  because that  $I_{CHSH}^{(1)}$  is always no more than  $I_{CHSH}^{(2)}$  in this region, and the setting of measurement directions may be same as the original proposal [34];
- if  $G > 0.8$ ,  $I_{CHSH}^{(2)}$  may be not greater than  $I_{CHSH}^{(1)}$  in that case, so they choose to consider raising the Bell-CHSH nonlocality sharing between Alice and Bob<sub>2</sub> by the increase of  $I_{CHSH}^{(2)}$ . Their analysis shows that the similarity of Bob<sub>1</sub>'s two measurement directions can raise the quantum correlation for the Alice–Bob<sub>2</sub> pair, and the measurement directions setting  $(\hat{\mu}/\hat{\nu})$  and  $(\hat{\mu}'/\hat{\nu}')$  for Bob<sub>1</sub>/Bob<sub>2</sub> is now written as

$$\begin{aligned} \hat{\mu} &= \cos \gamma X + \sin \gamma Z, & \hat{\mu}' &= \cos \gamma X - \sin \gamma Z, \\ \hat{\nu} &= \cos \delta X + \sin \delta Z, & \hat{\nu}' &= \cos \delta X - \sin \delta Z. \end{aligned} \quad (63)$$

Here,  $\gamma$  and  $\delta$  are in the range between 0 and  $\frac{\pi}{4}$ , determined by the measurement precision G. They also demonstrate their scheme in the optical experiment, where different

precision factors  $G$  and the corresponding measurement direction settings have been selected. They plot the two CHSH results in Figure 5b, and it clearly shows a double violation of Bell-CHSH inequality even when the value of  $G = 0.96$ , that is, the near-maximum strength unattainable ( $0.910 < G < 1$ ) using the origin protocol [34].

The other measurement protocol to certify sustained entanglement and nonlocality is proposed by Foletto et al. [118]. They design a sequential measurement scenario where the measurements performed and outcomes obtained previously decide on subsequent measurement choices. The history of a given measurement setting sequence and the corresponding observed results represent the evolution of an initial state, and the next task is to exhibit sustained entanglement at every possible branch of this tree-like evolutionary structure. In their theoretical model, Alice performs unsharp measurements sequentially, while, at first, it randomly chooses one of two measurement settings,  $A_0$  or  $A_1$  (sharpness  $\mu_1$ ), and the post-measurement state has four possible configurations for two observed outcomes ( $\pm 1$ ) for each measurement direction. Then, the second Alice applies a unitary transformation  $U_{A,2}$  to its system depending on its knowledge of the previous measurement setting and outcome data, and continues to randomly choose between measurements with sharpness  $\mu_2$ . The configuration for the state after Alice's second measurement also has four choices and can be written in a similar form to the first post-measurement state. The above process can continue analogically by using a suitable sharpness parameter  $\mu_k$  at each step  $k$ , and thus the measurement sequence achieved on Alice's side can be unbounded long. They point out that the above sequence can be interrupted at any  $k$ -th Alice for proving the entanglement and nonlocality still shared with Bob, which is the other part of an entangled state and measures projectively. In that time, Bob needs to know measurements and outcomes history for Alice<sub>1</sub>, Alice<sub>2</sub>, ..., and Alice<sub>k-1</sub> to define the unitary operation  $U_{B,k}$  and measurement directions on its side. For the experiments, they demonstrate a proof-of-concept optical implementation and certify that three Alices can share quantum correlations between a single Bob via violating the Bell-CHSH inequality or entanglement witnesses [119] using their protocol. Such a tree-like structure can theoretically continue indefinitely, but, in the experiment, they choose to set the stopping point after Alice<sub>3</sub>. This finding is important for quantum information tasks that require certified entanglement, a typical application of which is the generation of unbounded quantum random numbers. In 2021, the same group [120] reported experimental results for randomness extraction following the previous theoretical model [103], which is similar to the above protocol. They consider the imperfections in a realistic situation, add noise to the initial shared state, and conclude that the random extraction gain from increasing the number of measurements in the sequence is offset by bringing in depolarization noise, even if it is small. In order to take advantage of the long sequence, the prepared state should be as close to the ideal case as possible. They verify the feasibility of certified randomness for imperfect preparation through the long-exposure test on the optical platform and compare the measured data with the predicted value of the theoretical model (Table 1). The two rightmost columns of the table indicate that the min-entropy  $H_{min,k}$  measured in the experiment is slightly lower than the predicted value, which is attributed to the systematic misalignment in the experimental setup. This work lays the foundation for higher-precision experimental setups in the next stage.

**Table 1.** Comparison of experimental measurements and theoretical predictions data in the long-exposure feasibility tests [120].

Step $k$	Previous Outcome	Strength (Rad)	$H_{min,k}$ (Model) (Bits)	$H_{min,k}$ (Experiment) (Bits)
1	Not applicable	0.4	0.165	$0.13 \pm 0.002$
2	0	Projective	0.263	$0.38 \pm 0.04$
2	1	Projective	0.263	$0.13 \pm 0.02$
1	Not applicable	0.47	0.085	$0.057 \pm 0.002$
2	0	0.1	0.303	$0.32 \pm 0.02$
2	1	0.1	0.303	$0.25 \pm 0.02$
1	Not applicable	0.52	0.035	$0.005 \pm 0.001$
2	0	0.1	0.369	$0.38 \pm 0.02$
2	1	0.1	0.369	$0.33 \pm 0.01$

## 5. Discussion

The effective utilization of quantum resources is one of the main challenges in the current development of quantum technology, and many important advances have been achieved in the direction of how to recycle quantum correlations from the same source. The core of such research is to adjust the disturbance degree of the measurement process to the quantum state by designing different weak measurement sequences and deduce and verify that the quantum correlations of a single entangled pair can be shared among multiple independent observers so as to efficiently reuse this quantum resource. This possibility of realizing qubit cycling through the sequence of multiple independent observers has aroused great theoretical interest, and here we list the major developments in Table 2. These theoretical studies not only benefit from fundamental conceptual exploration in quantum physics but also have important application potential for quantum randomness extraction. Up to now, related experimental studies have focused on optical devices, which also provide important insights into photon-based quantum computing [121–123].

**Table 2.** Theoretical advances and challenges for quantum correlation recycling in sequential unsharp measurement scenarios.

Publication Time	Quantum Correlation Scenarios	Observer Type	One-Sided	Multi-Sided	Measurement Settings	Upper Bound Analysis	Ref
2015	Bell nonlocality	Alice–Bob	✓		Equal sharpness	Bell-CHSH inequality: 2 Bobs (unbiased input)/no limit (biased input)	[34]
2016	Bell nonlocality	Alice–Bob	✓		Equal sharpness	Bell-CHSH inequality: 2 Bobs (unbiased input)	[41]
2018	Entanglement	Alice–Bob	✓		Equal sharpness	Entanglement witness: 12 Bobs	[54]
2018	EPR steering	Alice–Bob	✓		Equal sharpness	2-settings CFFW inequality: 2 Bobs n-settings CJWR inequality: n Bobs	[62]
2019	EPR steering	Alice–Bob	✓		Equal sharpness	An isotropic entangled state of local dimension $d$ : $d/\log d$ Bobs	[65]
2019	Bell nonlocality	Alice–Bob	✓		Equal sharpness	n-settings local realist inequality: 2 Bobs (unbiased input)	[35]
2019	Standard/genuine nonlocality	Alice–Bob–Charlie	✓		Equal sharpness	Mermin inequality: 6 Charlies Svetlichny inequality: 2 Charlies (unbiased input)	[77]
2019	Preparation contextuality	Alice–Bob	✓		Equal sharpness	Nontrivial preparation noncontextual inequalities: unbounded Bobs	[93]
2020	Genuine Entanglement	Alice–Bob–Charlie	✓		Equal sharpness	Tripartite entanglement witness: 12 Charlies	[82]
2020	Bell nonlocality	Alice–Bob	✓		Unequal sharpness	Bell-CHSH inequality: unbounded Bobs	[94]
2021	Genuine nonlocality	Alice–Bob–Charlie	✓		Unequal sharpness	Svetlichny inequality: 2 Charlies	[95]
2021	Bell nonlocality	Alice–Bob		✓	Unequal sharpness	Bell-CHSH inequality: not applicable (unbiased input)	[96]
2022	Genuine Entanglement	N-qubit pair		✓	Unequal sharpness	Genuine multipartite entanglement witnesses: an unboundedly long sequence	[98]
2022	Entanglement	Alice–Bob		✓	Unequal sharpness	Entanglement witness: an unboundedly long sequence	[99]
2023	EPR steering	Alice–Bob		✓	Unequal sharpness	3-settings CJWR inequality: unbounded Alices and Bobs	[66]

Recently, a new study [124] has shown that it is possible to overcome the apparent inabilitys for projective measurement strategies in recycling quantum resources by introducing classical randomness, realizing the effective sharing of quantum correlations. Specifically, the above measurement scheme uses the shared randomness between entangled pairs to randomly combine three different projective measurement strategies for Bobs and achieve the recycling of Bell nonlocality represented by two sequential violations of the CHSH inequality. This work generalizes the form of measurement strategies for efficient recycling of quantum correlations and is also validated by specific experiments in optical systems [125] that do not require entanglement assistance. These works demonstrate that projective measurements are an effective resource for recycling Bell nonlocality and leave open questions about their application to other sequential quantum correlation recycling protocols.

## 6. Concluding Remarks and Outlook

In this review, we summarize the relevant theoretical and experimental progress for quantum correlation resource recycling via sequential measurements. These results lay the foundation for more quantum correlation sharing schemes with higher experimental operability in the next step, which is expected to be applied in the field of the quantum network [126–128] and quantum teleportation [129,130]. It can be predicted that, by designing suitable measurement strategies, i.e., the sequences of weak measurements with adjustable intensity and measurement settings or a combination of projective measurements that introduce randomness, the study for multi-observer sharing of quantum correlations will help to provide a deeper explanation of the interplay among quantum measurement, quantum correlation, and quantum resource recycling.

**Author Contributions:** Conceptualization, X.H.; validation, L.Z.; formal analysis, L.L., S.B., Z.T. and J.Y.; investigation, L.L., S.B., Z.T. and J.Y.; writing—review and editing, X.H.; supervision, X.H.; project administration, L.Z. All authors have read and agreed to the published version of the manuscript.

**Funding:** This research was funded by Talent Introduction Project of Zhejiang Shuren University (Grant No. 2022R017 and Grant No. 2023R044).

**Data Availability Statement:** All needed information is here.

**Conflicts of Interest:** The author declares no conflict of interest.

## References

1. Einstein, A.; Podolsky, B.; Rosen, N. Can Quantum-Mechanical Description of Physical Reality Be Considered Complete? *Phys. Rev.* **1935**, *47*, 777–780. [[CrossRef](#)]
2. Bell, J.S. On the Einstein Podolsky Rosen paradox. *Phys. Phys. Fiz.* **1964**, *1*, 195–200. [[CrossRef](#)]
3. Brunner, N.; Cavalcanti, D.; Pironio, S.; Scarani, V.; Wehner, S. Bell nonlocality. *Rev. Mod. Phys.* **2014**, *86*, 419–478. [[CrossRef](#)]
4. Cavalcanti, D.; Skrzypczyk, P. Quantum steering: A review with focus on semidefinite programming. *Rep. Prog. Phys.* **2016**, *80*, 024001. [[CrossRef](#)]
5. Doherty, A.C.; Parrilo, P.A.; Spedalieri, F.M. Distinguishing Separable and Entangled States. *Phys. Rev. Lett.* **2002**, *88*, 187904. [[CrossRef](#)]
6. Pusey, M.F. Negativity and steering: A stronger Peres conjecture. *Phys. Rev. A* **2013**, *88*, 032313. [[CrossRef](#)]
7. Gühne, O.; Tóth, G. Entanglement detection. *Phys. Rep.* **2009**, *474*, 1–75. [[CrossRef](#)]
8. Horodecki, R.; Horodecki, P.; Horodecki, M.; Horodecki, K. Quantum entanglement. *Rev. Mod. Phys.* **2009**, *81*, 865–942. [[CrossRef](#)]
9. Bera, A.; Das, T.; Sadhukhan, D.; Roy, S.S.; De, A.S.; Sen, U. Quantum discord and its allies: A review of recent progress. *Reports on Progress in Physics* **2017**, *81*, 024001. [[CrossRef](#)]
10. Köhnke, S.; Agudelo, E.; Schünemann, M.; Schlettwein, O.; Vogel, W.; Sperling, J.; Hage, B. Quantum Correlations beyond Entanglement and Discord. *Phys. Rev. Lett.* **2021**, *126*, 170404. [[CrossRef](#)]
11. Simon Kochen, E.S. The Problem of Hidden Variables in Quantum Mechanics. *Indiana Univ. Math. J.* **1968**, *17*, 59–87. [[CrossRef](#)]
12. Bennett, C.H.; Brassard, G.; Crépeau, C.; Jozsa, R.; Peres, A.; Wootters, W.K. Teleporting an unknown quantum state via dual classical and Einstein-Podolsky-Rosen channels. *Phys. Rev. Lett.* **1993**, *70*, 1895–1899. [[CrossRef](#)] [[PubMed](#)]
13. Ekert, A.K. Quantum cryptography based on Bell’s theorem. *Phys. Rev. Lett.* **1991**, *67*, 661–663. [[CrossRef](#)] [[PubMed](#)]
14. Bennett, C.H.; Wiesner, S.J. Communication via one- and two-particle operators on Einstein-Podolsky-Rosen states. *Phys. Rev. Lett.* **1992**, *69*, 2881–2884. [[CrossRef](#)] [[PubMed](#)]

15. Li, C.L.; Fu, Y.; Liu, W.B.; Xie, Y.M.; Li, B.H.; Zhou, M.G.; Yin, H.L.; Chen, Z.B. Breaking the rate-distance limitation of measurement-device-independent quantum secret sharing. *Phys. Rev. Res.* **2023**, *5*, 033077. [\[CrossRef\]](#)

16. Yin, H.L.; Fu, Y.; Li, C.L.; Weng, C.X.; Li, B.H.; Gu, J.; Lu, Y.S.; Huang, S.; Chen, Z.B. Experimental quantum secure network with digital signatures and encryption. *Natl. Sci. Rev.* **2023**, *10*, nwac228. [\[CrossRef\]](#) [\[PubMed\]](#)

17. Li, C.L.; Fu, Y.; Liu, W.B.; Xie, Y.M.; Li, B.H.; Zhou, M.G.; Yin, H.L.; Chen, Z.B. Breaking universal limitations on quantum conference key agreement without quantum memory. *Commun. Phys.* **2023**, *6*, 122. [\[CrossRef\]](#)

18. Murao, M.; Jonathan, D.; Plenio, M.B.; Vedral, V. Quantum telecloning and multiparticle entanglement. *Phys. Rev. A* **1999**, *59*, 156–161. [\[CrossRef\]](#)

19. Hillery, M.; Bužek, V.; Berthiaume, A. Quantum secret sharing. *Phys. Rev. A* **1999**, *59*, 1829–1834. [\[CrossRef\]](#)

20. Scarani, V.; Gisin, N. Quantum Communication between  $N$  Partners and Bell’s Inequalities. *Phys. Rev. Lett.* **2001**, *87*, 117901. [\[CrossRef\]](#)

21. Zhao, Z.; Chen, Y.A.; Zhang, A.N.; Yang, T.; Briegel, H.J.; Pan, J.W. Experimental demonstration of five-photon entanglement and open-destination teleportation. *Nature* **2004**, *430*, 54–58. [\[CrossRef\]](#)

22. Coffman, V.; Kundu, J.; Wootters, W.K. Distributed entanglement. *Phys. Rev. A* **2000**, *61*, 052306. [\[CrossRef\]](#)

23. Toner, B.; Verstraete, F. Monogamy of Bell correlations and Tsirelson’s bound. *arXiv* **2006**, arXiv:quant-ph/quant-ph/0611001.

24. Reid, M.D. Monogamy inequalities for the Einstein-Podolsky-Rosen paradox and quantum steering. *Phys. Rev. A* **2013**, *88*, 062108. [\[CrossRef\]](#)

25. Lami, L.; Hirche, C.; Adesso, G.; Winter, A. Schur Complement Inequalities for Covariance Matrices and Monogamy of Quantum Correlations. *Phys. Rev. Lett.* **2016**, *117*, 220502. [\[CrossRef\]](#)

26. Heisenberg, W. *The Physical Principles of the Quantum Theory*; Courier Corporation: North Chelmsford, MA, USA, 1949.

27. Von Neumann, J. *Mathematical Foundations of Quantum Mechanics: New Edition*; Princeton University Press: Princeton, NJ, USA, 2018; Volume 53.

28. Aharonov, Y.; Bergmann, P.G.; Lebowitz, J.L. Time Symmetry in the Quantum Process of Measurement. *Phys. Rev.* **1964**, *134*, B1410–B1416. [\[CrossRef\]](#)

29. Aharonov, Y.; Albert, D.Z.; Vaidman, L. How the result of a measurement of a component of the spin of a spin-1/2 particle can turn out to be 100. *Phys. Rev. Lett.* **1988**, *60*, 1351–1354. [\[CrossRef\]](#)

30. Duck, I.M.; Stevenson, P.M.; Sudarshan, E.C.G. The sense in which a “weak measurement” of a spin-1/2 particle’s spin component yields a value 100. *Phys. Rev. D* **1989**, *40*, 2112–2117. [\[CrossRef\]](#)

31. Sciarrino, F.; Ricci, M.; De Martini, F.; Filip, R.; Mišta, L. Realization of a Minimal Disturbance Quantum Measurement. *Phys. Rev. Lett.* **2006**, *96*, 020408. [\[CrossRef\]](#)

32. Fuchs, C.A.; Peres, A. Quantum-state disturbance versus information gain: Uncertainty relations for quantum information. *Phys. Rev. A* **1996**, *53*, 2038–2045. [\[CrossRef\]](#)

33. Buscemi, F.; Horodecki, M. Towards a Unified Approach to Information-Disturbance Tradeoffs in Quantum Measurements. *Open Syst. Inf. Dyn.* **2009**, *16*, 29–48. [\[CrossRef\]](#)

34. Silva, R.; Gisin, N.; Guryanova, Y.; Popescu, S. Multiple Observers Can Share the Nonlocality of Half of an Entangled Pair by Using Optimal Weak Measurements. *Phys. Rev. Lett.* **2015**, *114*, 250401. [\[CrossRef\]](#) [\[PubMed\]](#)

35. Das, D.; Ghosal, A.; Sasmal, S.; Mal, S.; Majumdar, A.S. Facets of bipartite nonlocality sharing by multiple observers via sequential measurements. *Phys. Rev. A* **2019**, *99*, 022305. [\[CrossRef\]](#)

36. Herrero-Collantes, M.; Garcia-Escartin, J.C. Quantum random number generators. *Rev. Mod. Phys.* **2017**, *89*, 015004. [\[CrossRef\]](#)

37. Ma, X.; Yuan, X.; Cao, Z.; Qi, B.; Zhang, Z. Quantum random number generation. *npj Quantum Inf.* **2016**, *2*, 1–9. [\[CrossRef\]](#)

38. Pironio, S.; Acín, A.; Massar, S.; de La Giroday, A.B.; Matsukevich, D.N.; Maunz, P.; Olmschenk, S.; Hayes, D.; Luo, L.; Manning, T.A.; et al. Random numbers certified by Bell’s theorem. *Nature* **2010**, *464*, 1021–1024. [\[CrossRef\]](#)

39. Stipšić, P.; Milivojević, M. Control of a spin qubit in a lateral GaAs quantum dot based on symmetry of gating potential. *Phys. Rev. B* **2020**, *101*, 165302. [\[CrossRef\]](#)

40. Stavrou, V.N. Spin qubits: Spin relaxation in coupled quantum dots. *J. Phys. Condens. Matter* **2018**, *30*, 455301. [\[CrossRef\]](#)

41. Mal, S.; Majumdar, A.S.; Home, D. Sharing of nonlocality of a single member of an entangled pair of qubits is not possible by more than two unbiased observers on the other wing. *Mathematics* **2016**, *4*, 48. [\[CrossRef\]](#)

42. Busch, P.; Lahti, P.J.; Mittelstaedt, P. *The Quantum Theory of Measurement*; Springer: Berlin/Heidelberg, Germany, 1996.

43. Busch, P.; Grabowski, M.; Lahti, P.J. *Operational Quantum Physics*; Springer Science & Business Media: Berlin/Heidelberg, Germany, 1997; Volume 31.

44. Nielsen, M.A.; Chuang, I.L. *Quantum Computation and Quantum Information*; Cambridge University Press: Cambridge, UK, 2010.

45. Davies, E.B.; Lewis, J.T. An operational approach to quantum probability. *Commun. Math. Phys.* **1970**, *17*, 239–260. [\[CrossRef\]](#)

46. Gelfand, I.; Neumark, M. On the imbedding of normed rings into the ring of operators in Hilbert space. *Rec. Math. [Mat. Sbornik] N.S.* **1943**, *12*, 197–217.

47. Peres, A. Neumark’s theorem and quantum inseparability. *Found. Phys.* **1990**, *20*, 1441–1453. [\[CrossRef\]](#)

48. Peres, A. *Quantum Theory: Concepts and Methods*; Springer: Berlin/Heidelberg, Germany, 1997; Volume 72.

49. Schrödinger, E. Die gegenwärtige Situation in der Quantenmechanik. *Naturwissenschaften* **1935**, *23*, 844–849. [\[CrossRef\]](#)

50. Clauser, J.F.; Horne, M.A.; Shimony, A.; Holt, R.A. Proposed Experiment to Test Local Hidden-Variable Theories. *Phys. Rev. Lett.* **1969**, *23*, 880–884. [\[CrossRef\]](#)

51. Busch, P. Indeterminacy relations and simultaneous measurements in quantum theory. *Int. J. Theor. Phys.* **1985**, *24*, 63–92. [\[CrossRef\]](#)

52. Busch, P. Unsharp reality and joint measurements for spin observables. *Phys. Rev. D* **1986**, *33*, 2253–2261. [\[CrossRef\]](#) [\[PubMed\]](#)

53. Ren, C.; Feng, T.; Yao, D.; Shi, H.; Chen, J.; Zhou, X. Passive and active nonlocality sharing for a two-qubit system via weak measurements. *Phys. Rev. A* **2019**, *100*, 052121. [\[CrossRef\]](#)

54. Bera, A.; Mal, S.; De, A.S.; Sen, U. Witnessing bipartite entanglement sequentially by multiple observers. *Phys. Rev. A* **2018**, *98*, 062304. [\[CrossRef\]](#)

55. Horodecki, M.; Horodecki, P.; Horodecki, R. Separability of mixed states: Necessary and sufficient conditions. *Phys. Lett. A* **1996**, *223*, 1–8. [\[CrossRef\]](#)

56. Woronowicz, S. Nonextendible positive maps. *Commun. Math. Phys.* **1976**, *51*, 243–282. [\[CrossRef\]](#)

57. Lewenstein, M.; Kraus, B.; Cirac, J.I.; Horodecki, P. Optimization of entanglement witnesses. *Phys. Rev. A* **2000**, *62*, 052310. [\[CrossRef\]](#)

58. Bruß, D.; Cirac, J.I.; Horodecki, P.; Hulpke, F.; Kraus, B.; Lewenstein, M.; Sanpera, A. Reflections upon separability and distillability. *J. Mod. Opt.* **2002**, *49*, 1399–1418. [\[CrossRef\]](#)

59. Gühne, O.; Reimpell, M.; Werner, R.F. Estimating Entanglement Measures in Experiments. *Phys. Rev. Lett.* **2007**, *98*, 110502. [\[CrossRef\]](#) [\[PubMed\]](#)

60. Gühne, O.; Hyllus, P.; Bruß, D.; Ekert, A.; Lewenstein, M.; Macchiavello, C.; Sanpera, A. Experimental detection of entanglement via witness operators and local measurements. *J. Mod. Opt.* **2003**, *50*, 1079–1102. [\[CrossRef\]](#)

61. Werner, R.F. Quantum states with Einstein–Podolsky–Rosen correlations admitting a hidden-variable model. *Phys. Rev. A* **1989**, *40*, 4277–4281. [\[CrossRef\]](#)

62. Sasmal, S.; Das, D.; Mal, S.; Majumdar, A.S. Steering a single system sequentially by multiple observers. *Phys. Rev. A* **2018**, *98*, 012305. [\[CrossRef\]](#)

63. Cavalcanti, E.G.; Foster, C.J.; Fuwa, M.; Wiseman, H.M. Analog of the Clauser–Horne–Shimony–Holt inequality for steering. *JOSA B* **2015**, *32*, A74–A81. [\[CrossRef\]](#)

64. Cavalcanti, E.G.; Jones, S.J.; Wiseman, H.M.; Reid, M.D. Experimental criteria for steering and the Einstein–Podolsky–Rosen paradox. *Phys. Rev. A* **2009**, *80*, 032112. [\[CrossRef\]](#)

65. Shenoy H.A.; Designolle, S.; Hirsch, F.; Silva, R.; Gisin, N.; Brunner, N. Unbounded sequence of observers exhibiting Einstein–Podolsky–Rosen steering. *Phys. Rev. A* **2019**, *99*, 022317. [\[CrossRef\]](#)

66. Lv, Q.Q.; Liang, J.M.; Wang, Z.X.; Fei, S.M. Sharing EPR steering between sequential pairs of observers. *J. Phys. A Math. Theor.* **2023**, *56*, 325301. [\[CrossRef\]](#)

67. Pearle, P.M. Hidden-Variable Example Based upon Data Rejection. *Phys. Rev. D* **1970**, *2*, 1418–1425. [\[CrossRef\]](#)

68. Braunstein, S.L.; Caves, C.M. Wringing out better Bell inequalities. *Ann. Phys.* **1990**, *202*, 22–56. [\[CrossRef\]](#)

69. Gisin, N. Bell inequality for arbitrary many settings of the analyzers. *Phys. Lett. A* **1999**, *260*, 1–3. [\[CrossRef\]](#)

70. Collins, D.; Gisin, N. A relevant two qubit Bell inequality inequivalent to the CHSH inequality. *J. Phys. A Math. Gen.* **2004**, *37*, 1775. [\[CrossRef\]](#)

71. Deng, D.L.; Zhou, Z.S.; Chen, J.L. Relevant multi-setting tight Bell inequalities for qubits and qutrits. *Ann. Phys.* **2009**, *324*, 1996–2003. [\[CrossRef\]](#)

72. Brunner, N.; Gisin, N. Partial list of bipartite Bell inequalities with four binary settings. *Phys. Lett. A* **2008**, *372*, 3162–3167. [\[CrossRef\]](#)

73. Avis, D.; Imai, H.; Ito, T. On the relationship between convex bodies related to correlation experiments with dichotomic observables. *J. Phys. A Math. Gen.* **2006**, *39*, 11283. [\[CrossRef\]](#)

74. Gisin, N. Bell inequalities: Many questions, a few answers. *arXiv* **2009**, arXiv:quant-ph/0702021.

75. Hughston, L.P.; Jozsa, R.; Wootters, W.K. A complete classification of quantum ensembles having a given density matrix. *Phys. Lett. A* **1993**, *183*, 14–18. [\[CrossRef\]](#)

76. Hill, S.A.; Wootters, W.K. Entanglement of a Pair of Quantum Bits. *Phys. Rev. Lett.* **1997**, *78*, 5022–5025. [\[CrossRef\]](#)

77. Saha, S.; Das, D.; Sasmal, S.; Sarkar, D.; Mukherjee, K.; Roy, A.; Bhattacharya, S.S. Sharing of tripartite nonlocality by multiple observers measuring sequentially at one side. *Quantum Inf. Process.* **2019**, *18*, 1–15. [\[CrossRef\]](#)

78. Mermin, N.D. Extreme quantum entanglement in a superposition of macroscopically distinct states. *Phys. Rev. Lett.* **1990**, *65*, 1838–1840. [\[CrossRef\]](#) [\[PubMed\]](#)

79. Svetlichny, G. Distinguishing three-body from two-body nonseparability by a Bell-type inequality. *Phys. Rev. D* **1987**, *35*, 3066–3069. [\[CrossRef\]](#) [\[PubMed\]](#)

80. Mermin, N.D. Simple unified form for the major no-hidden-variables theorems. *Phys. Rev. Lett.* **1990**, *65*, 3373–3376. [\[CrossRef\]](#) [\[PubMed\]](#)

81. Bancal, J.D.; Barrett, J.; Gisin, N.; Pironio, S. Definitions of multipartite nonlocality. *Phys. Rev. A* **2013**, *88*, 014102. [\[CrossRef\]](#)

82. Maity, A.G.; Das, D.; Ghosal, A.; Roy, A.; Majumdar, A.S. Detection of genuine tripartite entanglement by multiple sequential observers. *Phys. Rev. A* **2020**, *101*, 042340. [\[CrossRef\]](#)

83. Acín, A.; Bruß, D.; Lewenstein, M.; Sanpera, A. Classification of Mixed Three-Qubit States. *Phys. Rev. Lett.* **2001**, *87*, 040401. [\[CrossRef\]](#) [\[PubMed\]](#)

84. Bourennane, M.; Eibl, M.; Kurtsiefer, C.; Gaertner, S.; Weinfurter, H.; Gühne, O.; Hyllus, P.; Bruß, D.; Lewenstein, M.; Sanpera, A. Experimental Detection of Multipartite Entanglement using Witness Operators. *Phys. Rev. Lett.* **2004**, *92*, 087902. [\[CrossRef\]](#)

85. Bruß, D. Characterizing entanglement. *J. Math. Phys.* **2002**, *43*, 4237–4251. [\[CrossRef\]](#)

86. Sørensen, A.S.; Mølmer, K. Entanglement and Extreme Spin Squeezing. *Phys. Rev. Lett.* **2001**, *86*, 4431–4434. [\[CrossRef\]](#)

87. Tóth, G. Multipartite entanglement and high-precision metrology. *Phys. Rev. A* **2012**, *85*, 022322. [\[CrossRef\]](#)

88. Seevinck, M.; Uffink, J. Partial separability and entanglement criteria for multiqubit quantum states. *Phys. Rev. A* **2008**, *78*, 032101. [\[CrossRef\]](#)

89. Lu, C.Y.; Zhou, X.Q.; Gühne, O.; Gao, W.B.; Zhang, J.; Yuan, Z.S.; Goebel, A.; Yang, T.; Pan, J.W. Experimental entanglement of six photons in graph states. *Nat. Phys.* **2007**, *3*, 91–95. [\[CrossRef\]](#)

90. Roos, C.F.; Riebe, M.; Haffner, H.; Hansel, W.; Benhelm, J.; Lancaster, G.P.; Becher, C.; Schmidt-Kaler, F.; Blatt, R. Control and measurement of three-qubit entangled states. *Science* **2004**, *304*, 1478–1480. [\[CrossRef\]](#)

91. Cabello, A. Experimentally Testable State-Independent Quantum Contextuality. *Phys. Rev. Lett.* **2008**, *101*, 210401. [\[CrossRef\]](#)

92. Mermin, N.D. Hidden variables and the two theorems of John Bell. *Rev. Mod. Phys.* **1993**, *65*, 803–815. [\[CrossRef\]](#)

93. Kumari, A.; Pan, A.K. Sharing nonlocality and nontrivial preparation contextuality using the same family of Bell expressions. *Phys. Rev. A* **2019**, *100*, 062130. [\[CrossRef\]](#)

94. Brown, P.J.; Colbeck, R. Arbitrarily Many Independent Observers Can Share the Nonlocality of a Single Maximally Entangled Qubit Pair. *Phys. Rev. Lett.* **2020**, *125*, 090401. [\[CrossRef\]](#)

95. Zhang, T.; Fei, S.M. Sharing quantum nonlocality and genuine nonlocality with independent observables. *Phys. Rev. A* **2021**, *103*, 032216. [\[CrossRef\]](#)

96. Cheng, S.; Liu, L.; Baker, T.J.; Hall, M.J.W. Limitations on sharing Bell nonlocality between sequential pairs of observers. *Phys. Rev. A* **2021**, *104*, L060201. [\[CrossRef\]](#)

97. Cheng, S.; Liu, L.; Baker, T.J.; Hall, M.J.W. Recycling qubits for the generation of Bell nonlocality between independent sequential observers. *Phys. Rev. A* **2022**, *105*, 022411. [\[CrossRef\]](#)

98. Srivastava, C.; Pandit, M.; Sen, U. Sequential detection of genuine multipartite entanglement is unbounded for entire hierarchy of number of qubits recycled. *arXiv* **2022**, arXiv:2208.08435.

99. Pandit, M.; Srivastava, C.; Sen, U. Recycled entanglement detection by arbitrarily many sequential and independent pairs of observers. *Phys. Rev. A* **2022**, *106*, 032419. [\[CrossRef\]](#)

100. Srivastava, C.; Pandit, M.; Sen, U. Entanglement witnessing by arbitrarily many independent observers recycling a local quantum shared state. *Phys. Rev. A* **2022**, *105*, 062413. [\[CrossRef\]](#)

101. Shannon, C.E. Communication theory of secrecy systems. *Bell Syst. Tech. J.* **1949**, *28*, 656–715. [\[CrossRef\]](#)

102. Metropolis, N.; Ulam, S. The monte carlo method. *J. Am. Stat. Assoc.* **1949**, *44*, 335–341. . 10483310 [\[CrossRef\]](#)

103. Curchod, F.J.; Johansson, M.; Augusiak, R.; Hoban, M.J.; Wittek, P.; Acín, A. Unbounded randomness certification using sequences of measurements. *Phys. Rev. A* **2017**, *95*, 020102. [\[CrossRef\]](#)

104. D’Ariano, G.M.; Presti, P.L.; Perinotti, P. Classical randomness in quantum measurements. *J. Phys. A Math. Gen.* **2005**, *38*, 5979. [\[CrossRef\]](#)

105. Acín, A.; Pironio, S.; Vértesi, T.; Wittek, P. Optimal randomness certification from one entangled bit. *Phys. Rev. A* **2016**, *93*, 040102. [\[CrossRef\]](#)

106. Coyle, B.; Hoban, M.J.; Kashefi, E. One-sided device-independent certification of unbounded random numbers. *arXiv* **2018**, arXiv:1806.10565. [\[CrossRef\]](#)

107. Bowles, J.; Baccari, F.; Salavvros, A. Bounding sets of sequential quantum correlations and device-independent randomness certification. *Quantum* **2020**, *4*, 344. [\[CrossRef\]](#)

108. Navascués, M.; Pironio, S.; Acín, A. Bounding the Set of Quantum Correlations. *Phys. Rev. Lett.* **2007**, *98*, 010401. [\[CrossRef\]](#)

109. Navascués, M.; Pironio, S.; Acín, A. A convergent hierarchy of semidefinite programs characterizing the set of quantum correlations. *New J. Phys.* **2008**, *10*, 073013. [\[CrossRef\]](#)

110. Schiavon, M.; Calderaro, L.; Pittaluga, M.; Vallone, G.; Villoresi, P. Three-observer Bell inequality violation on a two-qubit entangled state. *Quantum Sci. Technol.* **2017**, *2*, 015010. [\[CrossRef\]](#)

111. Kim, T.; Fiorentino, M.; Wong, F.N.C. Phase-stable source of polarization-entangled photons using a polarization Sagnac interferometer. *Phys. Rev. A* **2006**, *73*, 012316. [\[CrossRef\]](#)

112. Hu, M.J.; Zhou, Z.Y.; Hu, X.M.; Li, C.F.; Guo, G.C.; Zhang, Y.S. Observation of non-locality sharing among three observers with one entangled pair via optimal weak measurement. *npj Quantum Inf.* **2018**, *4*, 63. [\[CrossRef\]](#)

113. Choi, Y.H.; Hong, S.; Pramanik, T.; Lim, H.T.; Kim, Y.S.; Jung, H.; Han, S.W.; Moon, S.; Cho, Y.W. Demonstration of simultaneous quantum steering by multiple observers via sequential weak measurements. *Optica* **2020**, *7*, 675–679. [\[CrossRef\]](#)

114. Kwon, O.; Cho, Y.W.; Kim, Y.H. Single-mode coupling efficiencies of type-II spontaneous parametric down-conversion: Collinear, noncollinear, and beamlike phase matching. *Phys. Rev. A* **2008**, *78*, 053825. [\[CrossRef\]](#)

115. Zhu, J.; Hu, M.J.; Li, C.F.; Guo, G.C.; Zhang, Y.S. Einstein-Podolsky-Rosen steering in two-sided sequential measurements with one entangled pair. *Phys. Rev. A* **2022**, *105*, 032211. [\[CrossRef\]](#)

116. Anwer, H.; Wilson, N.; Silva, R.; Muhammad, S.; Tavakoli, A.; Bourennane, M. Noise-robust preparation contextuality shared between any number of observers via unsharp measurements. *Quantum* **2021**, *5*, 551. [\[CrossRef\]](#)

117. Feng, T.; Ren, C.; Tian, Y.; Luo, M.; Shi, H.; Chen, J.; Zhou, X. Observation of nonlocality sharing via not-so-weak measurements. *Phys. Rev. A* **2020**, *102*, 032220. [\[CrossRef\]](#)

118. Foletto, G.; Calderaro, L.; Tavakoli, A.; Schiavon, M.; Picciariello, F.; Cabello, A.; Villoresi, P.; Vallone, G. Experimental Certification of Sustained Entanglement and Nonlocality after Sequential Measurements. *Phys. Rev. Appl.* **2020**, *13*, 044008. [\[CrossRef\]](#)

119. Tóth, G.; Gühne, O. Detecting Genuine Multipartite Entanglement with Two Local Measurements. *Phys. Rev. Lett.* **2005**, *94*, 060501. [\[CrossRef\]](#)

120. Foletto, G.; Padovan, M.; Avesani, M.; Tebyanian, H.; Villoresi, P.; Vallone, G. Experimental test of sequential weak measurements for certified quantum randomness extraction. *Phys. Rev. A* **2021**, *103*, 062206. [\[CrossRef\]](#)

121. Zhong, H.S.; Li, Y.; Li, W.; Peng, L.C.; Su, Z.E.; Hu, Y.; He, Y.M.; Ding, X.; Zhang, W.; Li, H.; et al. 12-Photon Entanglement and Scalable Scattershot Boson Sampling with Optimal Entangled-Photon Pairs from Parametric Down-Conversion. *Phys. Rev. Lett.* **2018**, *121*, 250505. [\[CrossRef\]](#)

122. Zu, C.; Wang, Y.X.; Deng, D.L.; Chang, X.Y.; Liu, K.; Hou, P.Y.; Yang, H.X.; Duan, L.M. State-Independent Experimental Test of Quantum Contextuality in an Indivisible System. *Phys. Rev. Lett.* **2012**, *109*, 150401. [\[CrossRef\]](#)

123. Kwon, O.; Park, K.K.; Ra, Y.S.; Kim, Y.S.; Kim, Y.H. Time-bin entangled photon pairs from spontaneous parametric down-conversion pumped by a cw multi-mode diode laser. *Opt. Express* **2013**, *21*, 25492–25500. [\[CrossRef\]](#)

124. Steffinlongo, A.; Tavakoli, A. Projective Measurements Are Sufficient for Recycling Nonlocality. *Phys. Rev. Lett.* **2022**, *129*, 230402. [\[CrossRef\]](#)

125. Xiao, Y.; Rong, Y.X.; Han, X.H.; Wang, S.; Fan, X.; Li, W.C.; Gu, Y.J. Experimental recycling of Bell nonlocality with projective measurements. *arXiv* **2022**, arXiv:2212.03815. [\[CrossRef\]](#)

126. Mao, Y.L.; Li, Z.D.; Steffinlongo, A.; Guo, B.; Liu, B.; Xu, S.; Gisin, N.; Tavakoli, A.; Fan, J. Recycling nonlocality in a quantum network. *arXiv* **2022**, arXiv:2202.04840. [\[CrossRef\]](#)

127. Hou, W.; Liu, X.; Ren, C. Network nonlocality sharing via weak measurements in the extended bilocal scenario. *Phys. Rev. A* **2022**, *105*, 042436. [\[CrossRef\]](#)

128. Wang, J.H.; Wang, Y.J.; Wang, L.J.; Chen, Q. Network nonlocality sharing via weak measurements in the generalized star network configuration. *Phys. Rev. A* **2022**, *106*, 052412. [\[CrossRef\]](#)

129. Roy, S.; Bera, A.; Mal, S.; De, A.S.; Sen, U. Recycling the resource: Sequential usage of shared state in quantum teleportation with weak measurements. *Phys. Lett. A* **2021**, *392*, 127143. [\[CrossRef\]](#)

130. Das, S.; Halder, P.; Banerjee, R.; De, A.S. Sequential reattempt of telecloning. *Phys. Rev. A* **2023**, *107*, 042414. [\[CrossRef\]](#)

**Disclaimer/Publisher’s Note:** The statements, opinions and data contained in all publications are solely those of the individual author(s) and contributor(s) and not of MDPI and/or the editor(s). MDPI and/or the editor(s) disclaim responsibility for any injury to people or property resulting from any ideas, methods, instructions or products referred to in the content.